ENGINEERING AND INDUSTRIAL EXPERIMENT STATION

College of Engineering

University of Florida

STRUCTURE, PROPERTIES AND RADIATION SENSITIVITY OF ELECTRICALLY BISTABLE MATERIALS

Technical Report No. 4
6 February 1972

Second Annual Report
(ARPA DAHC04-70-C-0024)

ARPA Order Number:	1562
Program Code Number:	0D10
Name of Contractor:	University of Florida
Effective Date of Contract:	6 February 1970
Contract Expiration Date:	6 February 1973
Amount of Contract:	$137,816
Contract Number:	DAHC04-70-C-0024
Principal Investigator:	Dr. Derek B. Dove, Telephone 904-392-1497
Project Scientist:	Dr. Charles Boghosian, AROD, Telephone 919-286-2285

Sponsored by
Advanced Research Projects Agency
ARPA Order No. DAHC04-70-C-0024

STRUCTURE, PROPERTIES AND RADIATION SENSITIVITY OF ELECTRICALLY BISTABLE MATERIALS

Technical Report No. 4
6 February 1972

Submitted by

D. B. Dove, L. L. Hench,
R. W. Gould and R. E. Loehman
Department of Metallurgical and Materials Engineering
University of Florida
Gainesville, Florida 32601

Abstract

This second annual report describes work carried out on the structural and electrical characterization of chalcogenide glasses. Electron diffraction radial distribution studies have been completed in the $As_2Te_{3-x}Se_x$ system and the thermal stability of these glasses in the presence of metallic surface layers has been examined. X-ray measurements on the kinetics of crystallization of bulk $GeSe_x$ glasses have been continued and diffuse scattering data have been obtained on a number of Ge-Se-As bulk glasses. Glass transition and crystallization temperatures have been observed by differential scanning calorimetry, a technique of high sensitivity.

A comparison is made between the a.c. conductivity of glasses measured with planar and sandwich electrode configurations. A significant difference has been found which may be attributed to electrode polarization effects in the sandwich structure.

Finally, a simple technique employing the decomposition of molybdenum carbonyl is described for the rapid deposition of thick refractory electrodes of good conductivity.

TABLE OF CONTENTS

LOCAL ORDER IN AMORPHOUS FILMS OF As_2Te_3, As_2Te_2Se, As_2TeSe_2 and As_2Se_3

Electron Diffraction Studies

Films of several hundred Å in mean thickness have been prepared by flash evaporation of powdered bulk glass. Rock salt substrates at room temperature were used; films were stripped by water immersion and were picked up onto screening of several types. Electron diffraction intensity profiles were measured in the 50 kev scanning electron diffraction unit described in earlier reports.

Figures 1 through 4 show the intensity profiles for films of As_2Te_3, As_2Te_2Se, As_2TeSe_2 and As_2Se_3. Inelastic background has been removed experimentally by an electrostatic filter incorporated in the diffraction system. The curves show a pronounced peak at a small s value as noted earlier for Ge_xTe_{1-x} and Ge_xSe_{1-x} films. Figures 5 through 8 show the data after division by the square of the mean atomic scattering factor. The relative importance of the first halo in the intensity curve can be seen to be greatly diminished in these curves. Figure 9 shows the transforms of the si(s) curves (see for example report #3) taken over the range 0 to 1.8, where

$$i(s) = \frac{\text{Data}(s) - \overline{f_i^2}}{(\overline{f_i})^2} .$$

The computed curves a to d consist of a superposition of overlapping peaks weighted by factors depending on the types

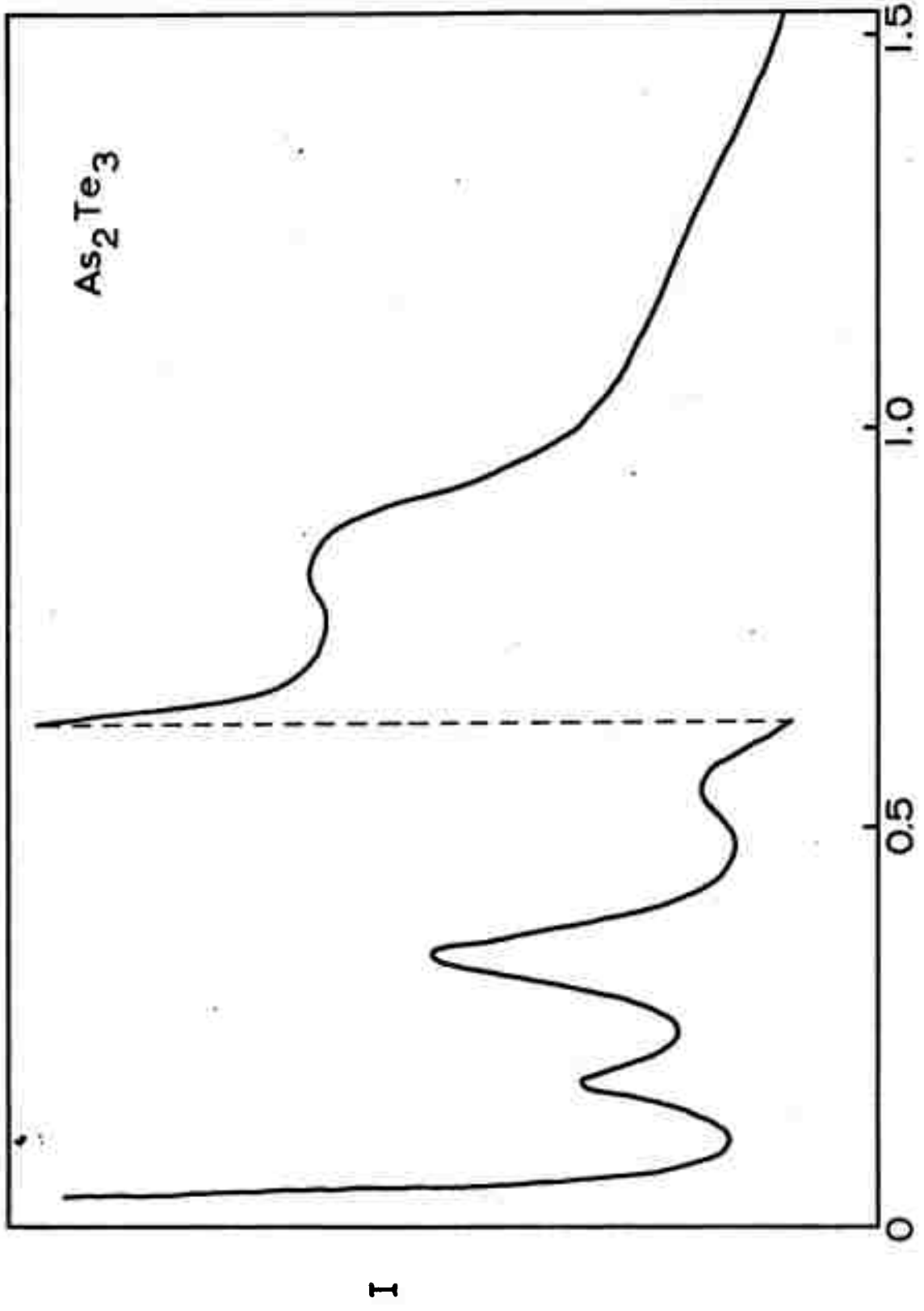

Fig. 1. Intensity versus scattering angle for As_2Te_3 film.

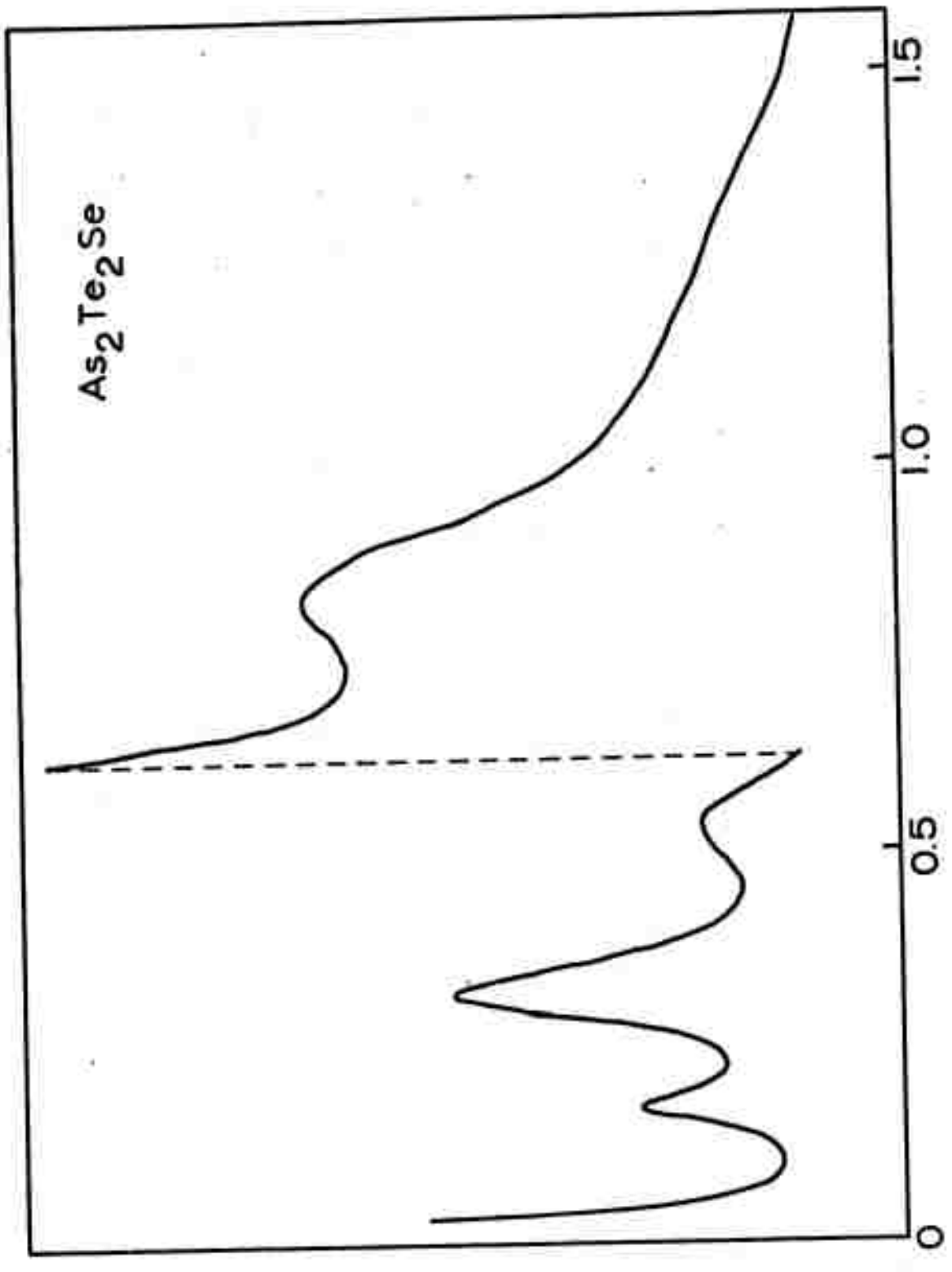

Fig. 2. Intensity versus scattering angle for As_2Te_2Se film.

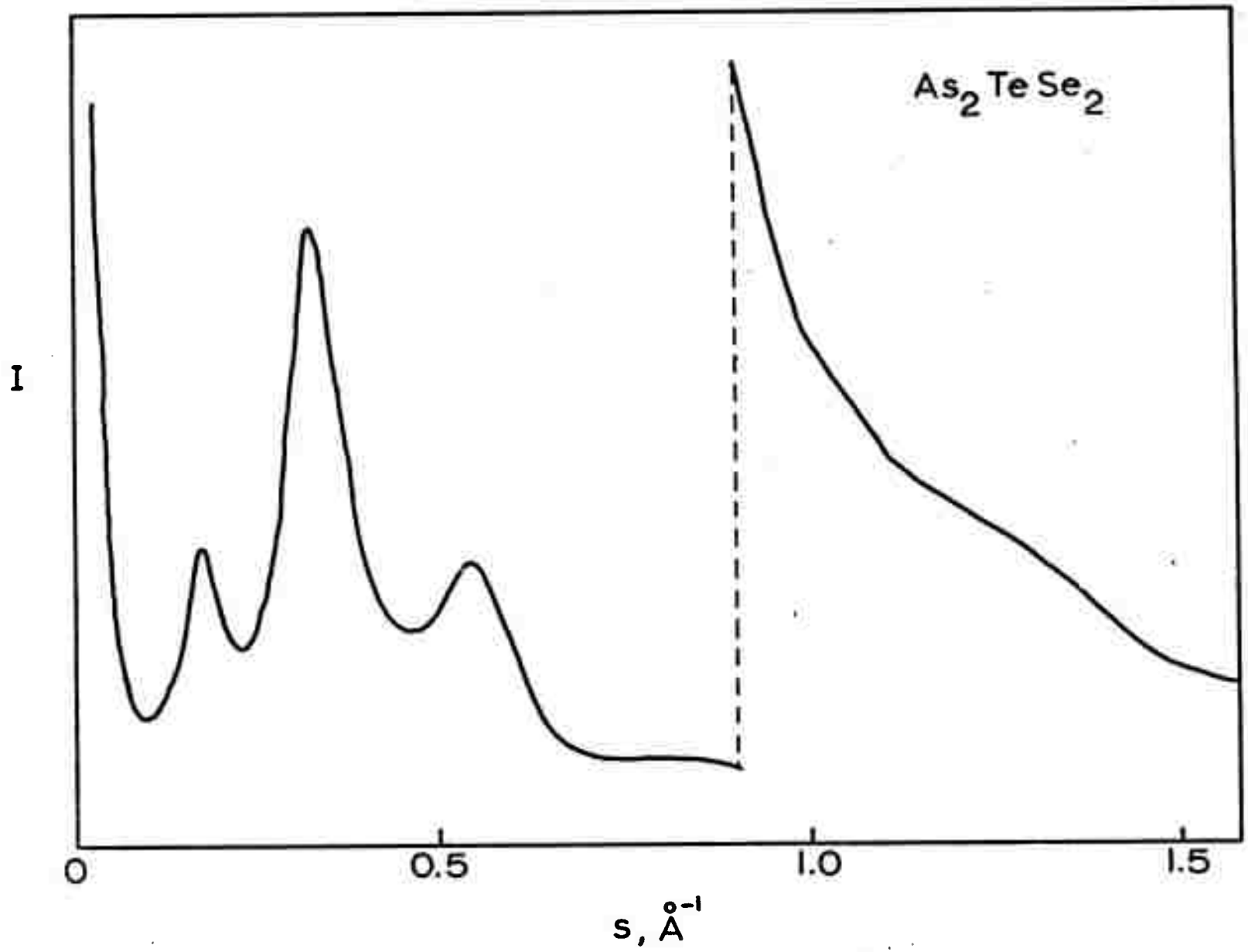

Fig. 3. Intensity versus scattering angle for As_2TeSe_2 film.

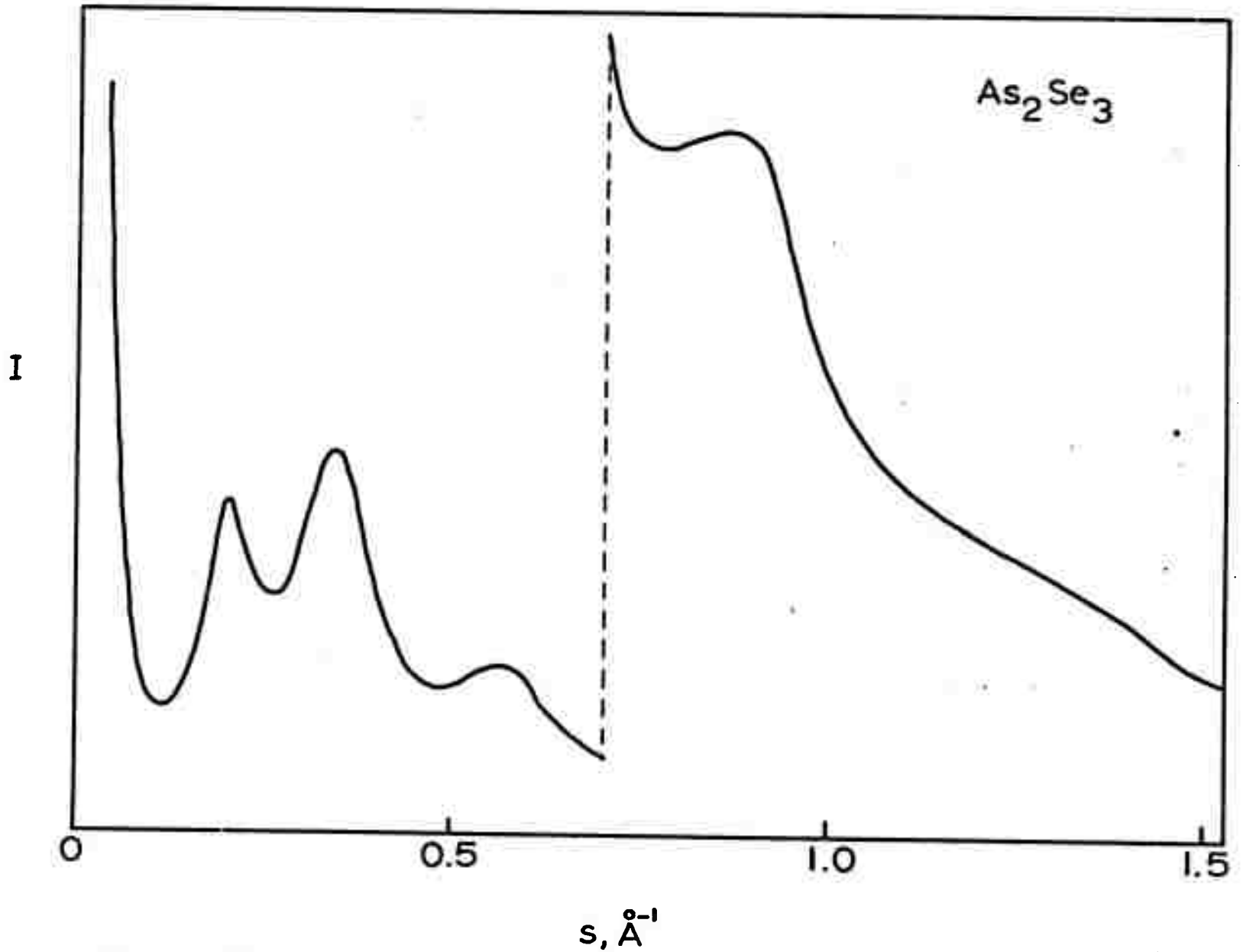

Fig. 4. Intensity versus scattering angle for As_2Se_3 film.

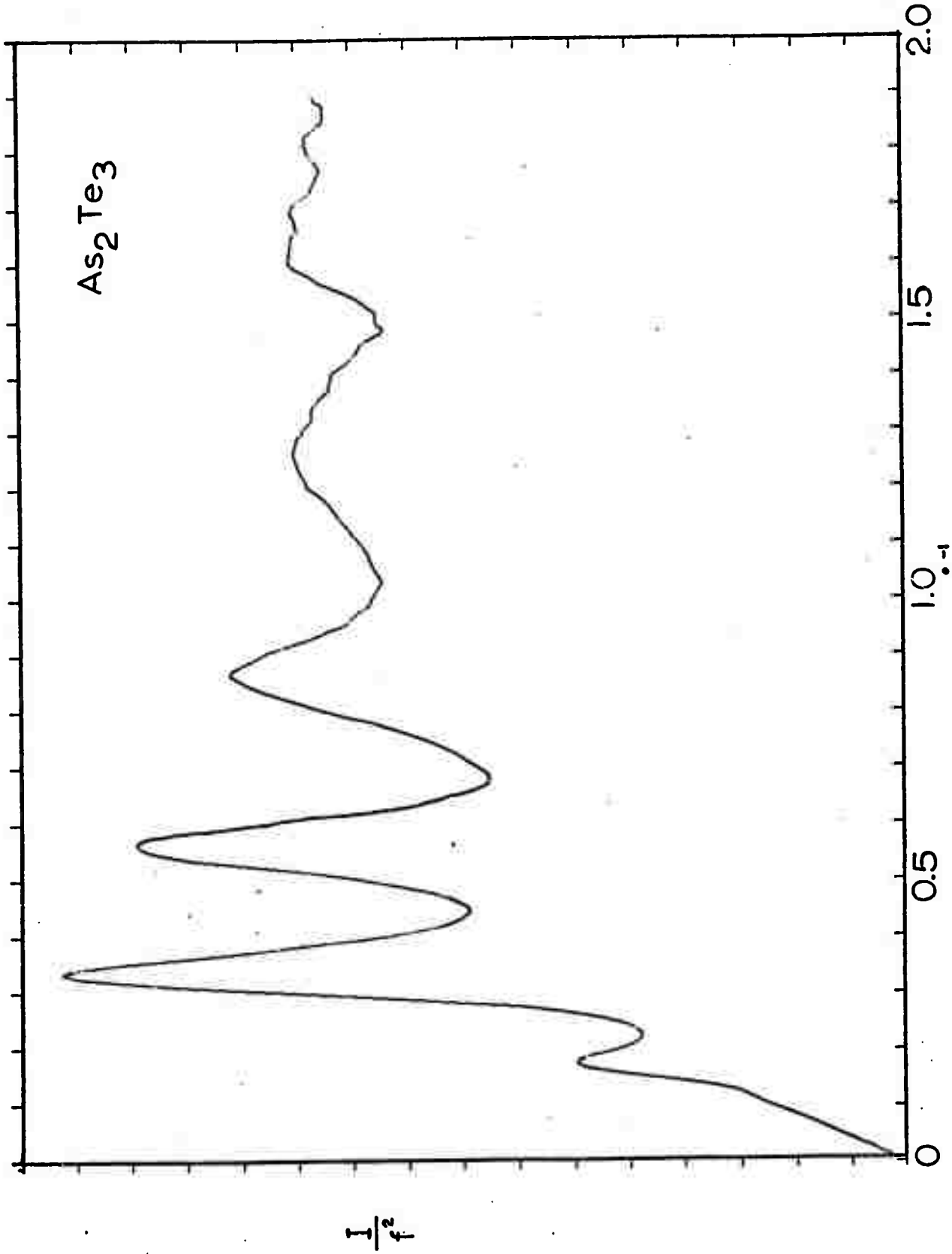

Fig. 5. Plot of I/f^2 for As_2Te_3.

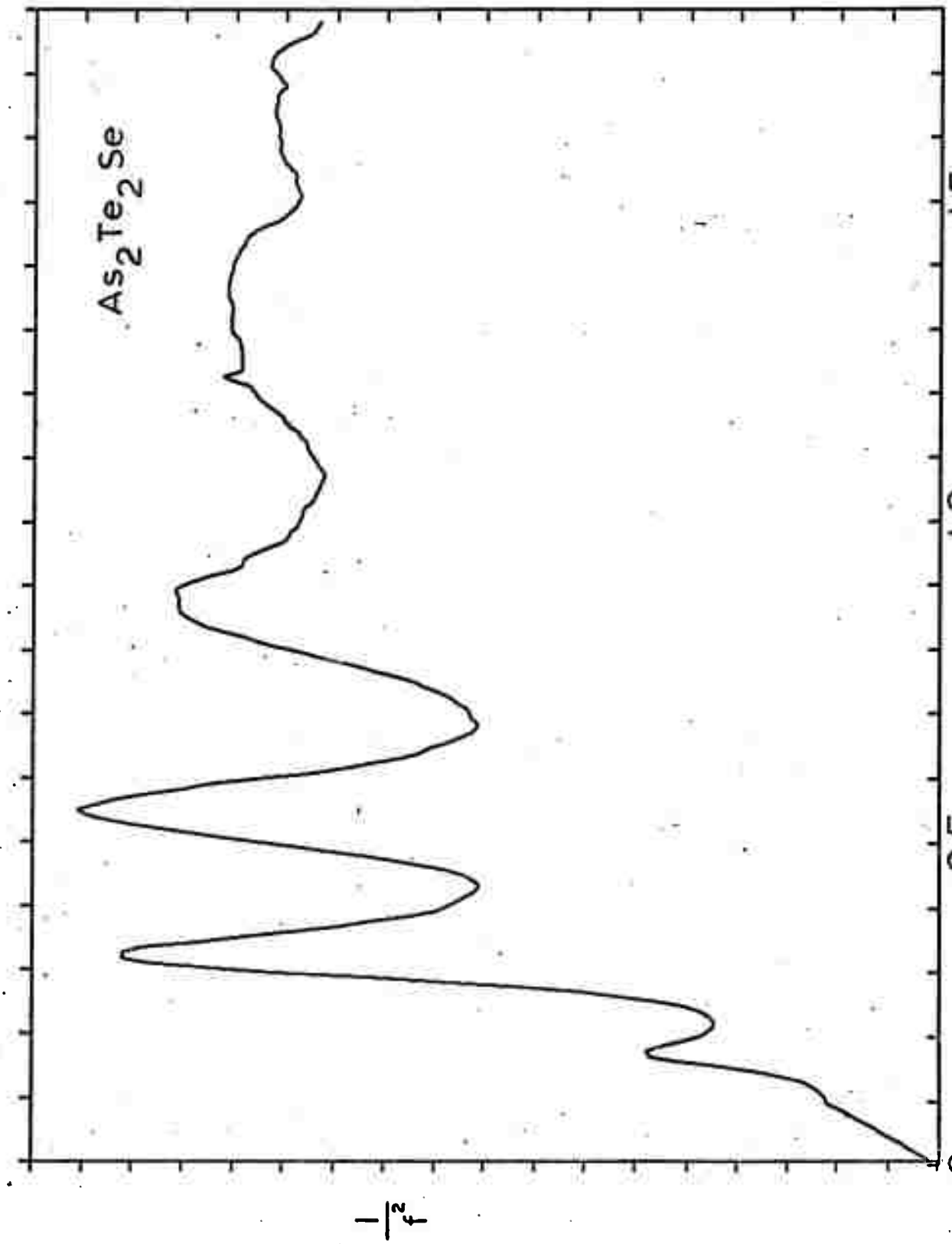

Fig. 6. Plot of I/f^2 for As_2Te_2Se.

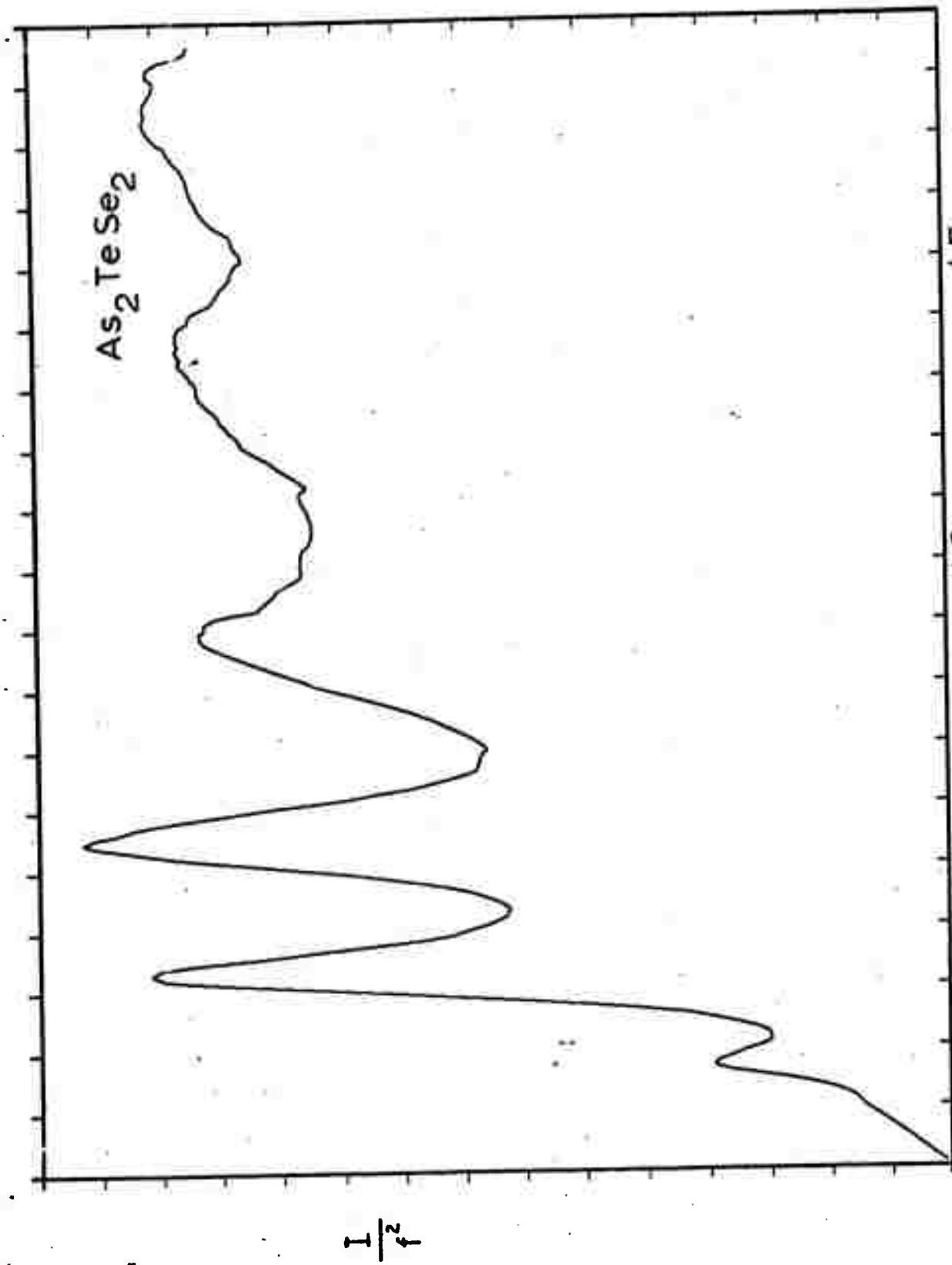

Fig. 7. Plot of I/f^2 for As_2TeSe_2.

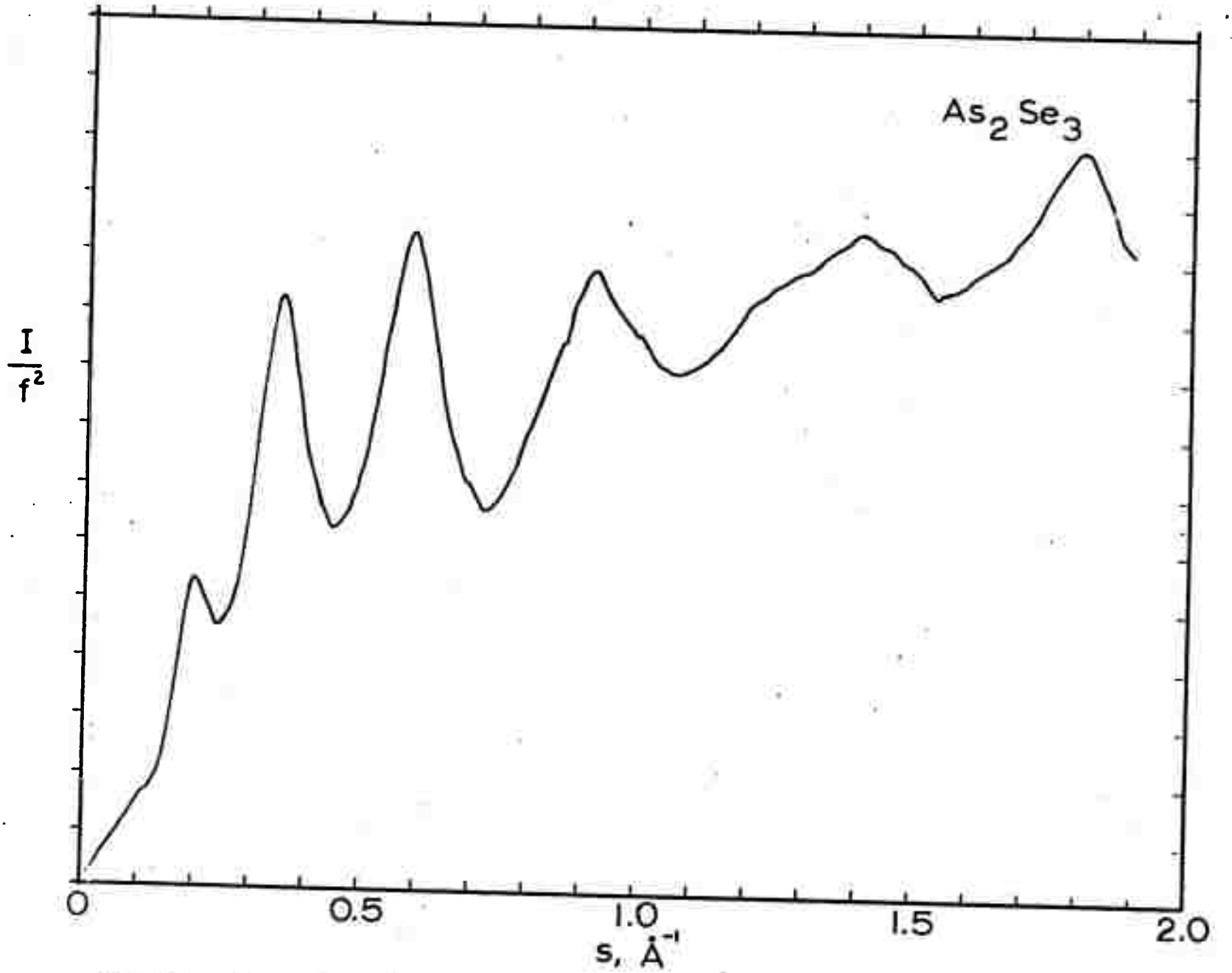

Fig. 8. Plot of I/f^2 for As_2Se_3.

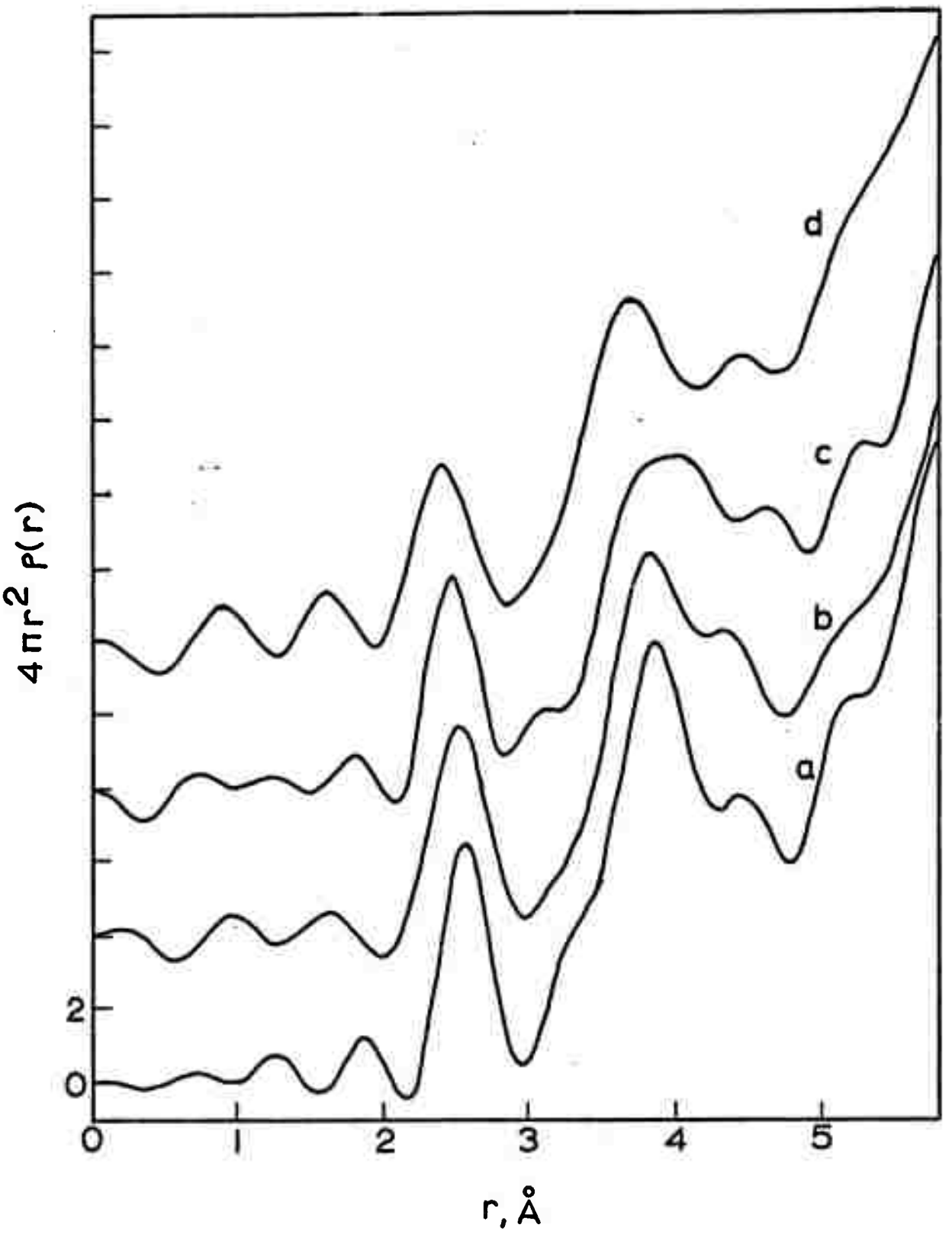

Fig. 9. Transform of the si(s) curves taken over s range 0.0 to 1.8. Curves a to d correspond to films of As_2Te_3, As_2Te_2Se, As_2TeSe_2, As_2Se_3 respectively.

of atoms involved and correspond to the compositions As_2Te_3, As_2Te_2Se, As_2TeSe_2 and As_2Se_3, respectively.

Examination of the first peak of these curves reveals a systematic variation in mean interatomic distance with composition as is to be expected. The area under the peak gives an approximate value for the average coordination number, the scattering factor corrections being small compared with experimental uncertainties. Table I summarizes this data.

Table I

Experimental mean of the nearest neighbor distances and mean coordination number

Film	Mean Peak Location	Area
As_2Te_3	2.57 Å	2.4
As_2Te_2Se	2.51 Å	2.5
As_2TeSe_2	2.47 Å	2.2
As_2Se_3	2.40 Å	2.1

The coordination number results are in accord with structural models in which three-fold and two-fold coordinations are assumed for the arsenic and chalcogen, respectively. The mean coordination for such models is equal to $(2 \times 3 + 3 \times 2)/5$, i.e., 2.4.

The results here are, however, at variance with those reported for As_2Te_3 and As_2Se_3 by Andrievskii et al.,* where very much larger coordination numbers were obtained. In this work, however, the films were described as 500 to 1,200 Å in thickness, an excessive thickness in our experience. In addition, ordinary photographic techniques were used with no possibility of removing inelastic background experimentally. The rdfs shown by these authors contain large negative regions and considerable ripple, making numerical values of areas under peaks very unreliable.

Two particular structural models may now be considered, one in which like atoms avoid each other, i.e., one in which compositional ordering occurs, and a second model in which bonds of different types occur randomly. Table II shows the relative numbers of different types of nearest neighbor bonds according to each model. No entry in this table indicates a zero.

Table III shows a list of interatomic distances found by simply summing covalent radii for the atoms concerned.**

Using Tables II and III it is possible to calculate the shape of the first peak in the rdf according to the two models. The results are shown in Figs. 10a and 10b. Thermal vibrational amplitudes have been taken to be independent

---

*A. I. Andrievskii, I. D. Nabitovich and Ya V. Voloshchuk, Sov. Phys. Cryst., 6, 534 (1962).

**L. Pauling, The Nature of the Chemical Bond, Cornell University Press, Ithaca, New York, 1960.

Table II

Fraction of bonds of different types in $As_2Te_{3-x}Se_x$ glasses calculated for random bonding (figure to left of square) and for ordered bonding (figure to right of square)

Bond Type	As_2Te_3	As_2Te_2Se	As_2TeSe_2	As_2Se_3
As-As	0.25	0.25	0.25	0.25
As-Te	0.50 / 1.00	0.33 / 0.67	0.17 / 0.33	
Te-Te	0.25	0.11	0.33	
Te-Se		0.11	0.03	
As-Se		0.17 / 0.33	0.11 / 0.67	0.50 / 1.00
Se-Se		0.03	0.11	0.25

Table III

Interatomic distances calculated from the sum of covalent radii

Bond Type	Å
Se-Se	2.32
Se-As	2.33
As-As	2.38
Se-Te	2.51
As-Te	2.54
Te-Te	2.70

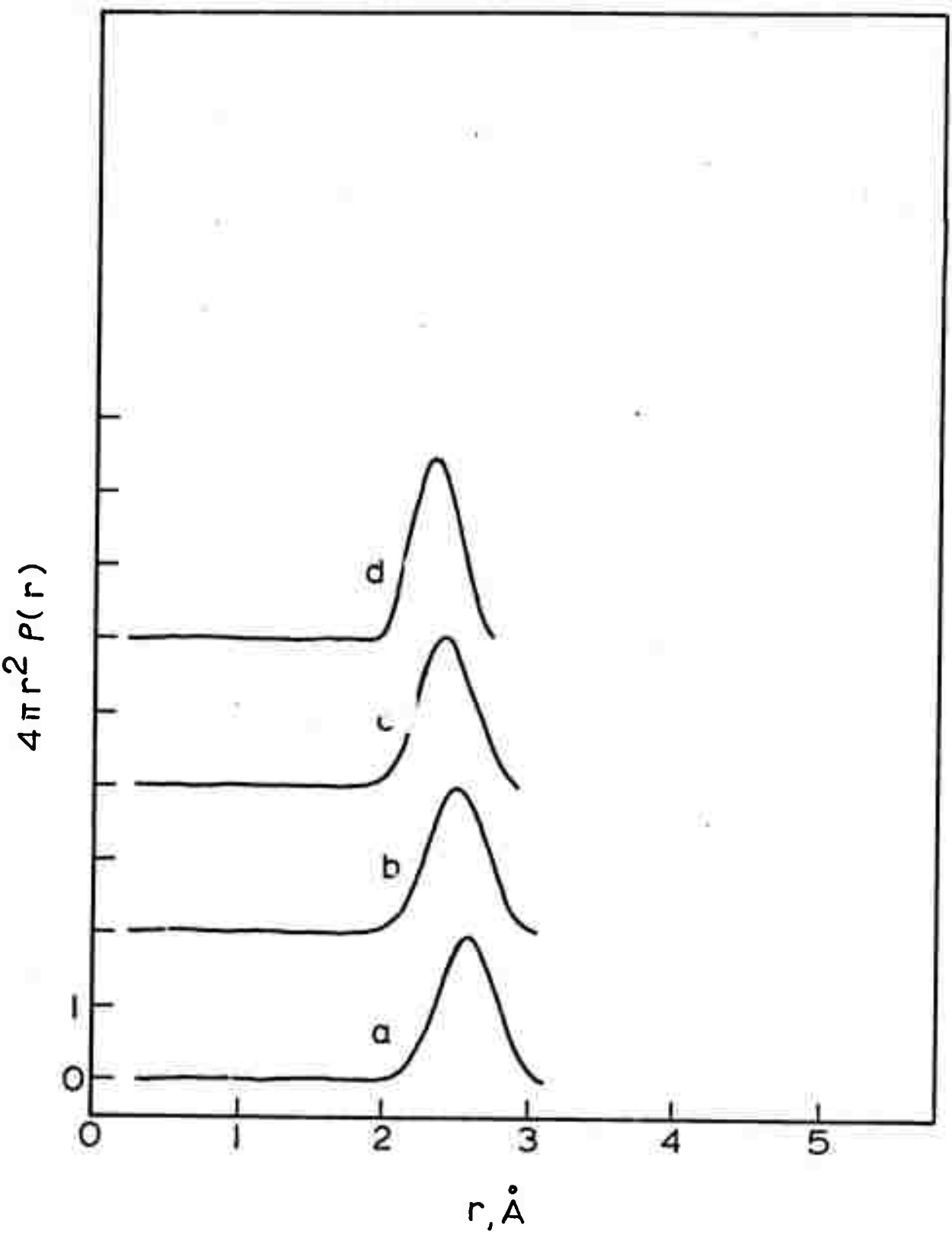

Fig. 10a. Calculated shape of the first peak in the rdf for randomly bonded model. Curves a to d correspond to the compositions As_2Te_3, As_2Te_2Se, As_2TeSe_2, As_2Se_3 respectively.

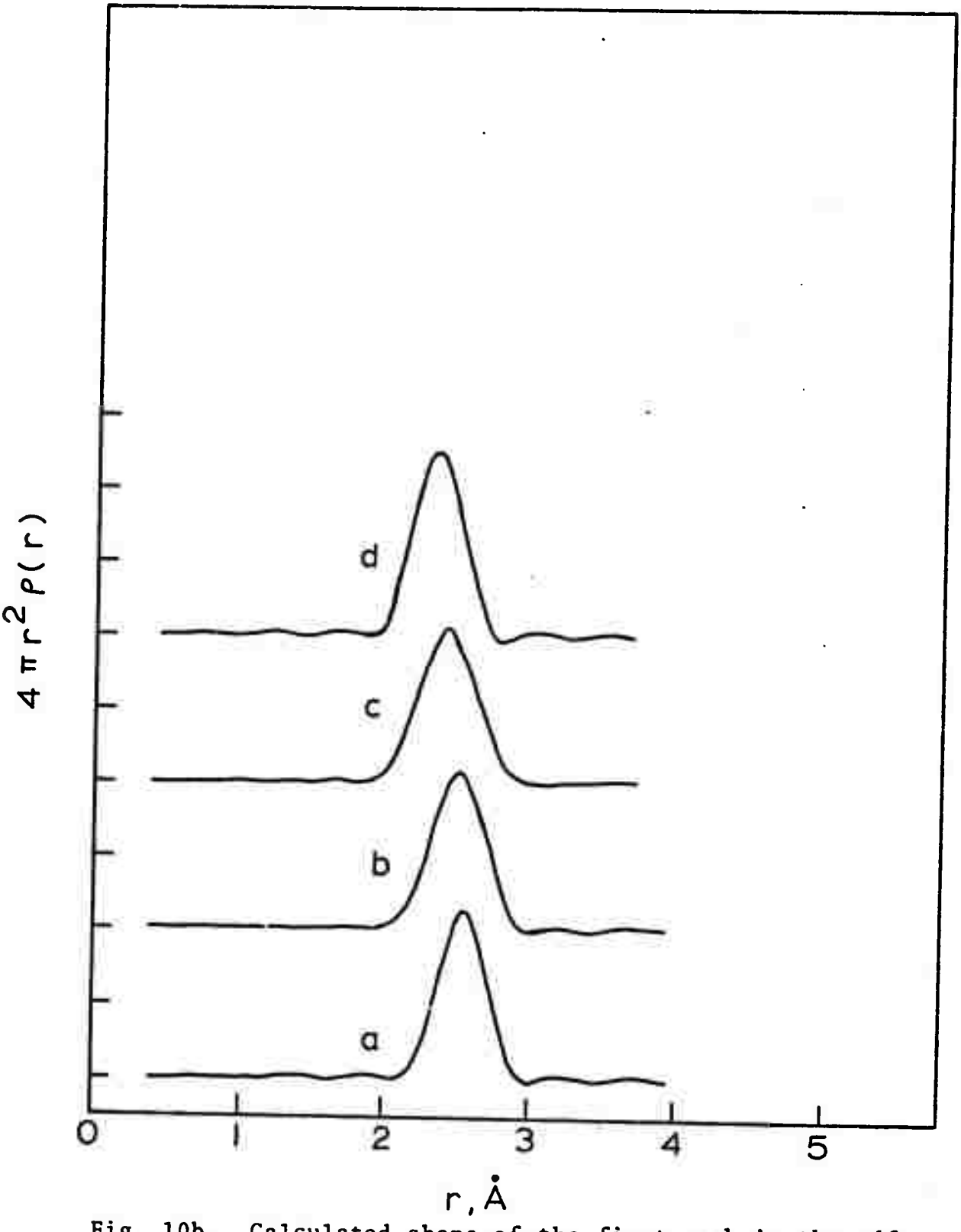

Fig. 10b. Calculated shape of the first peak in the rdf for compositionally ordered model. Curves a to d correspond to the compositions As_2Te_3, As_2Te_2Se, As_2TeSe_2, As_2Se_3 respectively.

of type of atom, an unrealistic approximation that may be improved in future work. Figures 10a and 10b show the systematic shift in mean peak position, in good agreement with experiment. It is hoped that peak shapes may be analyzed in more detail in order to decide which model provides the best fit to experiment. The results so far, however, indicate that very little difference in the shape of the first peak is to be expected between the two models.

EFFECT OF METALLIC ADDITIONS ON THERMAL STABILITY

As reported to various authors,* small amounts of metallic impurities may have a profound influence in promoting the devitrification of a glass. In earlier reports it was noted that structural charges could be readily brought about in Ge_xSe_{1-x} and Ge_xTe_{1-x} films, by heating in the electron diffraction system. It has been found that these effects are considerably influenced by the nature of the support mesh, thus copper mesh promotes structural changes while molybdenum mesh appears to have little effect.

Since impurity induced devitrification phenomena are likely to be of considerable importance for the stable operation of ovonic devices, some experiments have been carried

*See for example, Advances in Nucleation and Crystallization in Glasses, American Ceramic Society Symposium, L. L. Hench and S. W. Freiman (Eds.), 1971.

out to examine the influence of metallic impurities in more detail.

Amorphous films of As_2TeSe_2 have been heated in vacuum on several different types of support mesh, with and without the addition of metallic impurity. Heating rates were from 1 to 4°C/min approximately. Figure 11 shows a film heated on copper mesh inside the scanning electron diffraction system. Curves a to j were recorded after holding at temperature for a few minutes. The curves correspond to temperatures of 45, 61, 74, 94, 104, 109, 113, 123 and 151°C respectively. All heating was carried out using the heating stage of the Philips EM 200. The heating stage can be used interchangeably in the electron diffraction unit or in the electron microscope. Typically, heating was carried out in the electron diffraction unit and intensity profiles were recorded. The stage was then allowed to cool and was transferred to the electron microscope without disturbing the specimen. It was necessary, however, to expose the specimen to air during transfer and this must be taken into consideration.

The intensity profiles of the heated As_2TeSe_2 film show a remarkable similarity to those recorded previously for Ge_xSe_{1-x} and Ge_xTe_{1-x}. For comparison, films heated on molybdenum mesh showed no change in the shape of the intensity profile when heated in this way. Films frequently became mechanically unstable and broke up due to the somewhat larger grid size of the molybdenum mesh.

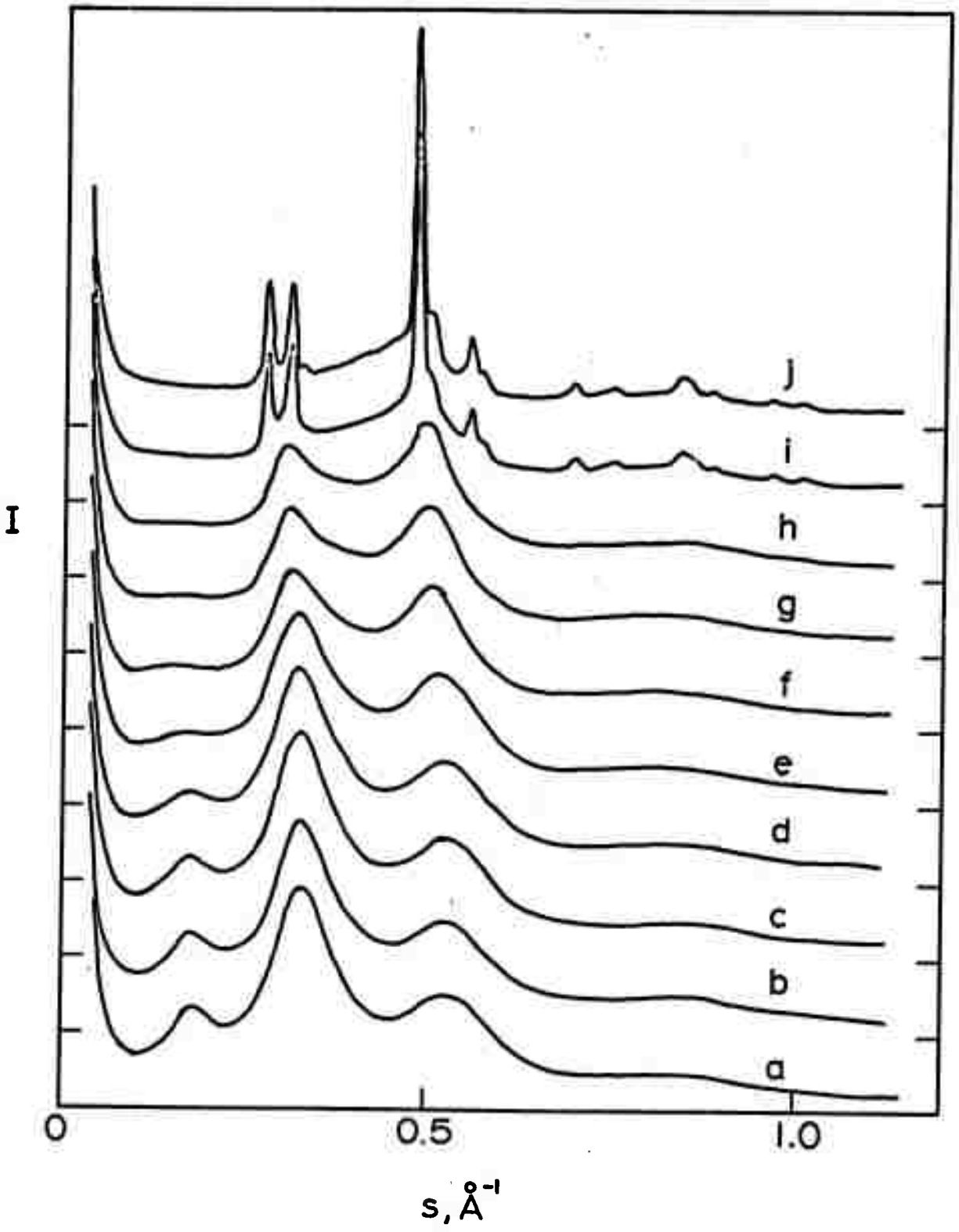

Fig. 11. Scans from As_2TeSe_2 after heating to various temperatures on copper support mesh. Curves a to j correspond to temperatures of 45, 61, 74, 94, 104, 109, 113, 123 and 151°C.

The copper mesh effect has some curious features. The structural changes do not start at the region of contact between mesh and film as may be anticipated. Instead, electron micrographs show a uniform distribution of small crystallites throughout the film when curve j has been reached, with little change in the film visible up to this point.

Figure 12 shows the result of using copper mesh that had been given a thin coating of molybdenum. Curve a is the as-prepared specimen. A thin layer of copper was deposited onto the film at room temperature inside the electron diffraction system. The intensity profile was remeasured and was found to have changed considerably as in curve b. The film was then removed from the diffraction system and examined in the electron microscope. The copper deposit could be clearly seen as very small particles on the featureless glassy film. Little direct indication of interaction between film and deposit could be seen.

The film was then replaced in the diffraction system and the room temperature intensity profile was recorded after a period of three days, resulting in curve c. The signs of peaks due to the copper deposit that were apparent in curve b had now disappeared. The film was then heated to 125°C, curve d, and 180°C, curve e, when crystallization commenced. In later electron micrographs it is clear that diffusion of copper had taken place; however, a direct crystallographic relationship between copper deposit, mesh or film crystallites could not be found.

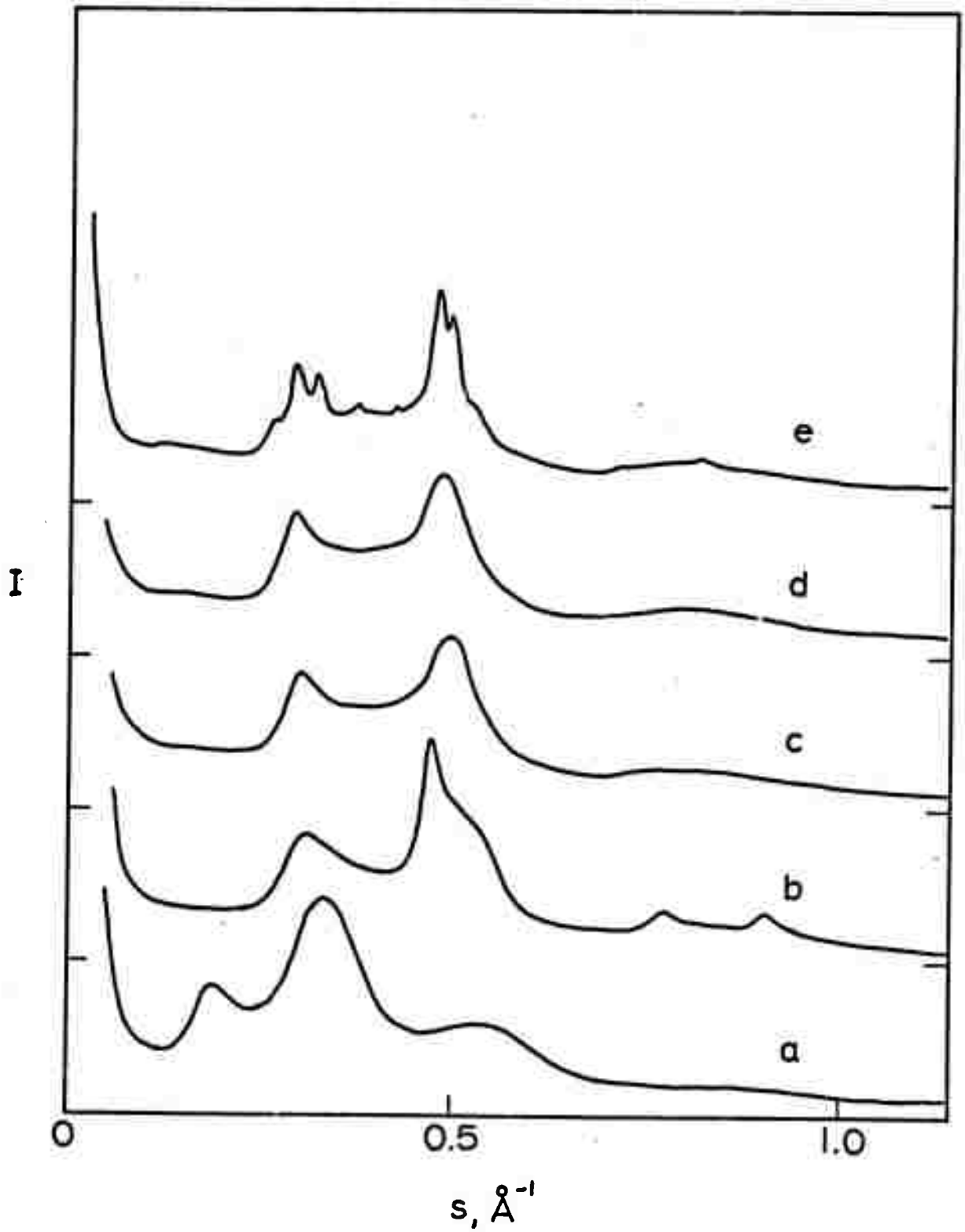

Fig. 12. Film of As_2TeSe_2 heated on a mesh of copper that had been given a thin coating of molybdenum. Curve a, as prepared; curve b, after deposition of a thin layer of Cu onto the film; curve c, after electron microscopic examination of film; curves d and e, after heating.

The experiment was repeated once more using molybdenum mesh. Figure 13 shows the result. Curve a is the intensity profile of an as-deposited film; curve b shows the result of depositing a very thin layer of copper inside the diffraction system. The curves d, e and f were recorded at higher gain and are from a carbon film placed in the system so that the profile of the copper deposit could be monitored. Curve d is the intensity profile of a very thin carbon layer, curve e was obtained after the copper deposition, and f after heating. The intensity profile has sharpened somewhat and has decreased in intensity due to some break-up of the film. Evidently, curve b simply shows the intensity contribution from the glassy film with the copper peaks superimposed. Heating to 220°C was necessary this time to bring out crystallization. The copper peaks have now disappeared and copper has diffused into or over the film as before.

In another experiment, aluminum was deposited onto a film on copper mesh thickly coated with molybdenum. Curve a of Fig. 14 shows the as-prepared glassy As_2TeSe_2 film. Curve b shows the result of adding a very thin deposit of aluminum. The curve is now a composite of the diffuse scattering from the glass and sharp diffraction peaks from the aluminum. Curve c shows the result of heating to 210°C. In this case, the aluminum peaks are still clearly visible and little interaction between the aluminum and the film was observed.

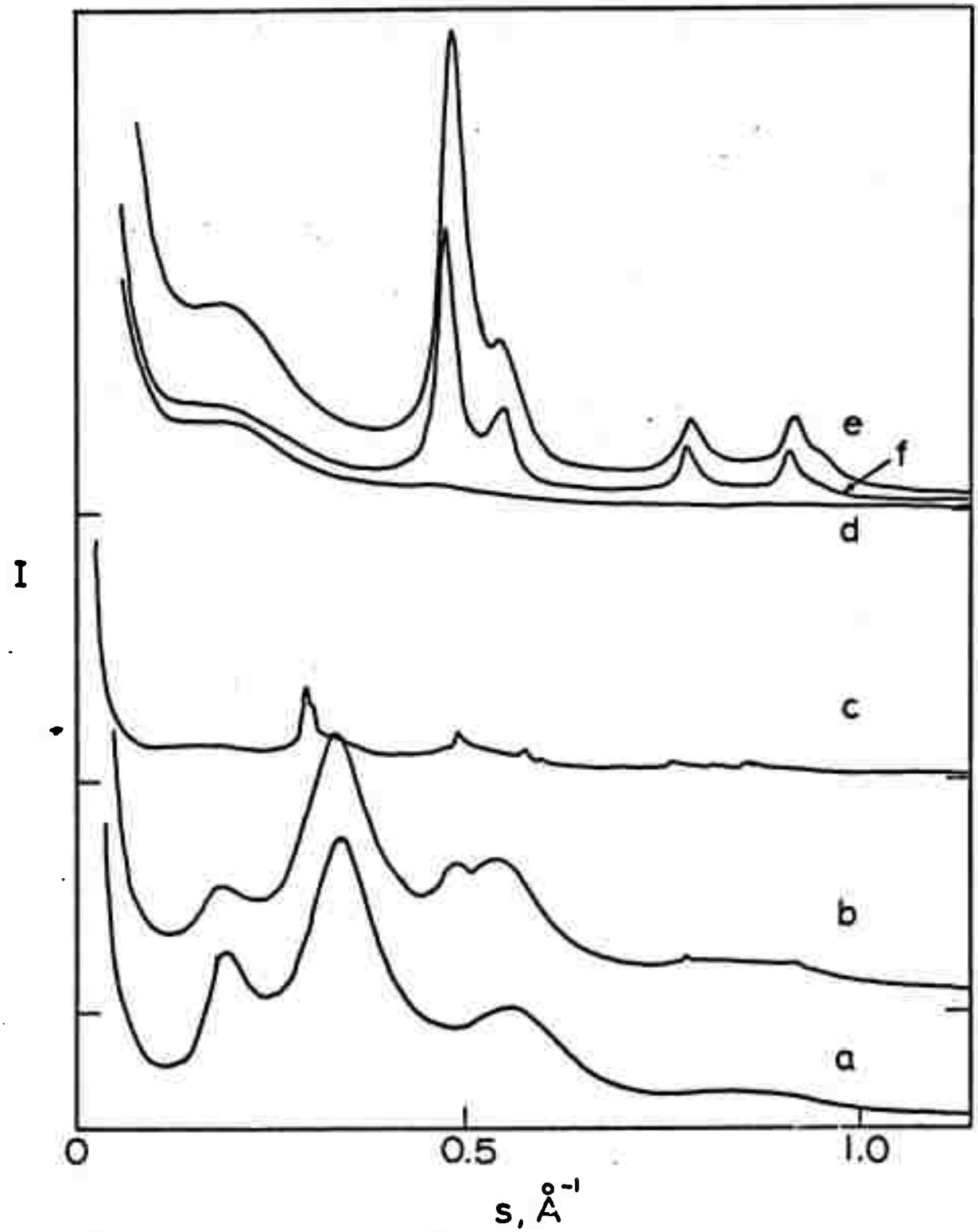

Fig. 13. Film of As_2TeSe_2 heated on a molybdenum mesh. Curve a, as prepared; curve b, after deposition of very thin layer of Cu; curve d is from a carbon monitor film; curves e and f show the carbon after deposition of copper and heat treatment.

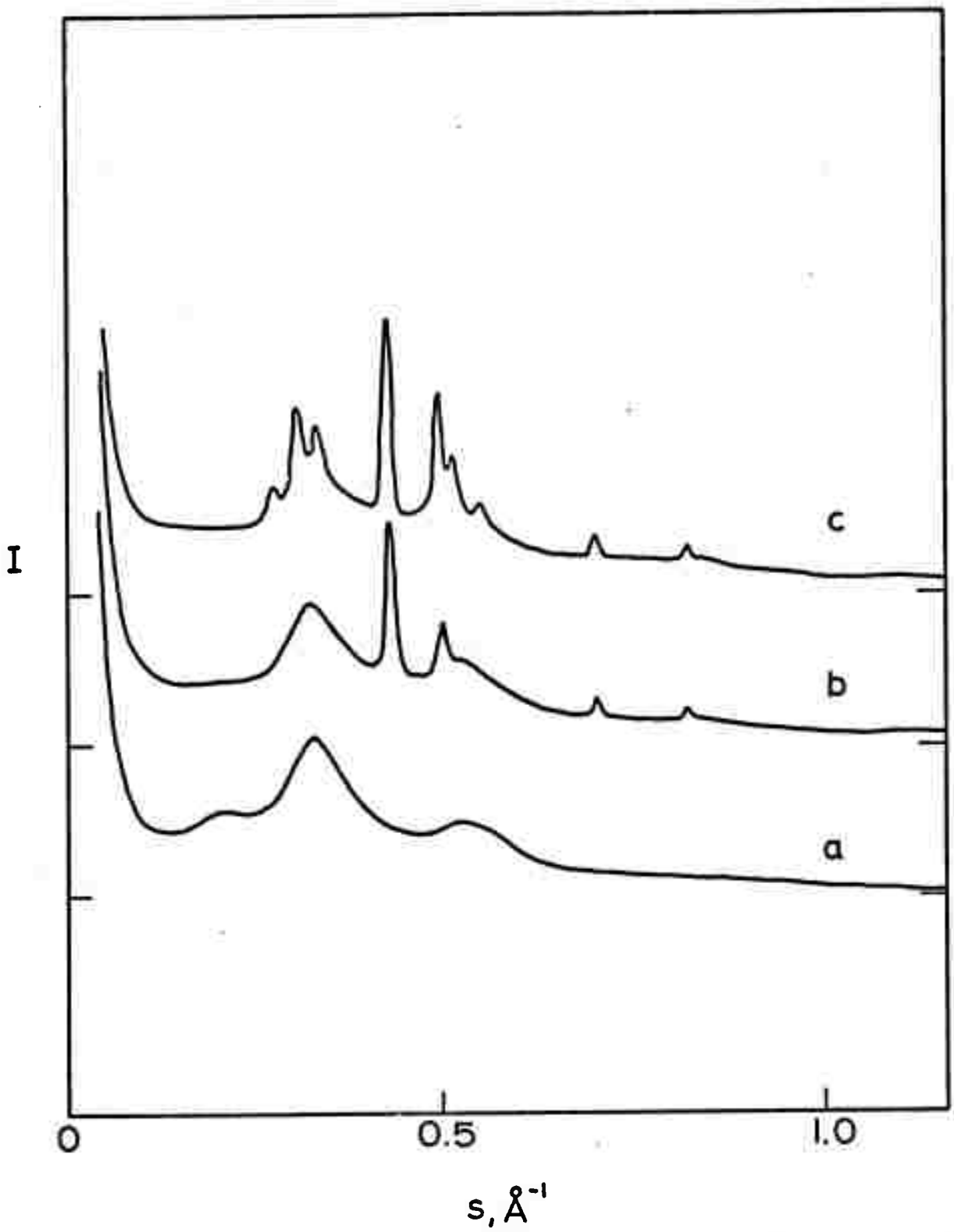

Fig. 14. Film of As_2TeSe_2 heated on a mesh of copper thickly coated with molybdenum. Curve a, as prepared; curve b, after deposition of a thin Al film; curve c shows result of heating to 210°C.

The films therefore appear to react very readily with copper via a diffusion mechanism to produce a glassy structural change at temperatures only slightly above room temperature. The films then crystallize at a somewhat lower temperature than untreated films.

Molybdenum and aluminum appear to have little effect.

Further work on impurity induced crystallization is in progress in view of its importance both for device operation and stability and for its significance in understanding diffusion and crystallization processes in amorphous solids.

X-RAY DIFFRACTION STUDIES OF BULK CHALCOGENIDES

X-ray investigations of bulk solids have been made in two general areas: 1) the kinetics of crystallization of binary $GeSe_x$ compounds, and 2) structural studies on a variety of binary and ternary chalcogenide glasses.

Sample preparation. Bulk samples of $GeSe_x$ and $Ge_xSe_yAs_z$ have been prepared by quenching from the melt. Seven to ten gram mixtures of the appropriate elements (99.99% purity or better) were sealed in 17 mm O.D. evacuated silica capsules. These capsules were heated with periodic agitation from 24 to 48 hours and then quenched in an ice-brine mixture.

Heat treatment. Approximately half-gram amounts of $GeSe_{1.5}$, $GeSe_{1.75}$, $GeSe_{2.0}$, $GeSe_{3.5}$ and $GeSe_4$ were sealed in evacuated Pyrex capsules and were heat treated at 475°±2°

for varying lengths of time. The samples were quenched to room temperature, and the samples were removed and ground to a 200 mesh powder.

X-ray diffraction procedure. The powders were analyzed for degree of crystallinity and identification of crystalline phases using a Norelco diffraction unit (CuKα radiation) with a scanning speed of 1° (2θ) per minute. The slit system parameters were 1°, 0.006 inches and 1°. The detector was a scintillation counter with a pulse height analyzer. The Scherrer technique was utilized to measure the size of the growing crystallites as a function of time and heat treatment. A more rigorous line profile analysis is underway and will be reported later.

Figures 15 and 16 show plots of the crystallization data for $GeSe_{1.5}$ at 475°C representing, respectively, the volume fraction of crystallites and crystallite size as a function of time. The curves are very similar to those reported earlier for low temperatures. It can be seen that growth rate is accelerated at higher temperatures as is to be expected. This work is in progress and will be reported more fully at a later date.

Amorphous scattering measurements. To prepare samples for the amorphous scattering measurements, powdered glass was placed in aluminum spectrographic caps and was pressed at 10,000 psi. Samples prepared in this manner were compared with large flat solid samples and were found to give essentially the same intensity curves. Powdered samples

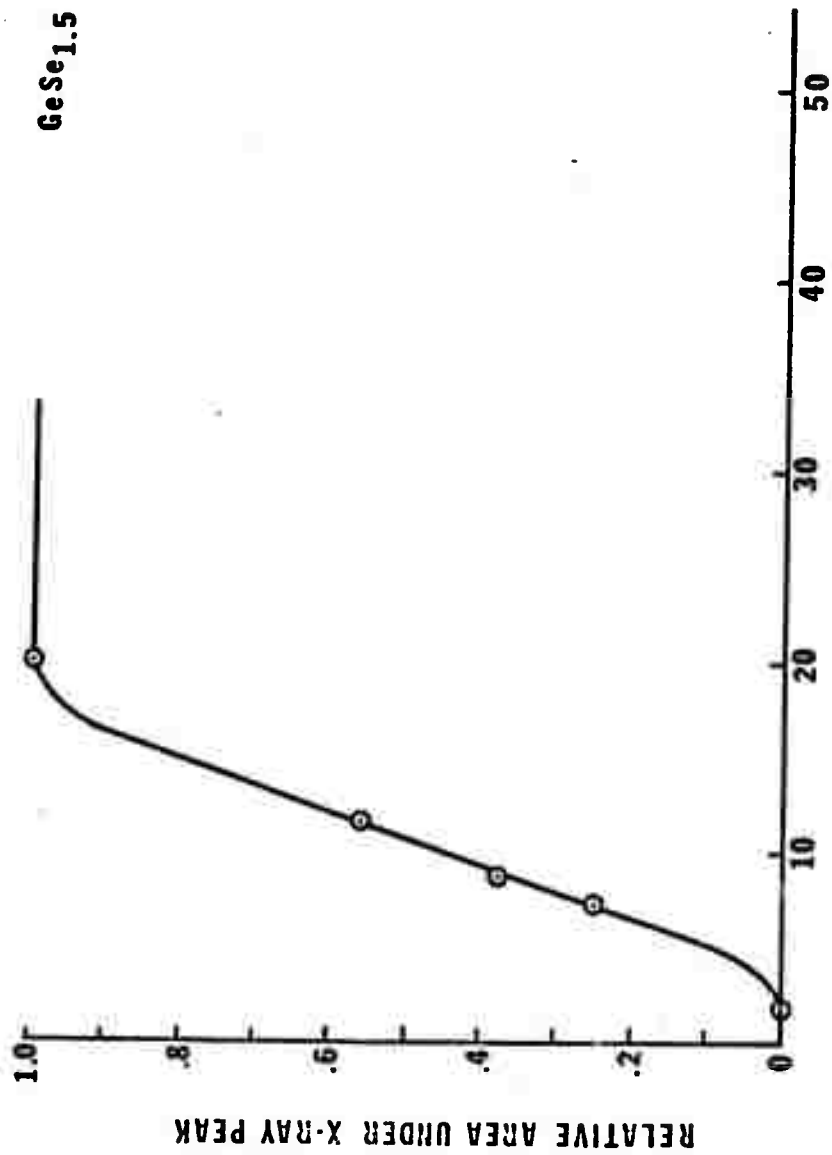

Fig. 15. Volume fraction of crystallites as a function of time from x-ray data of GeSe1.5 held at 475°C.

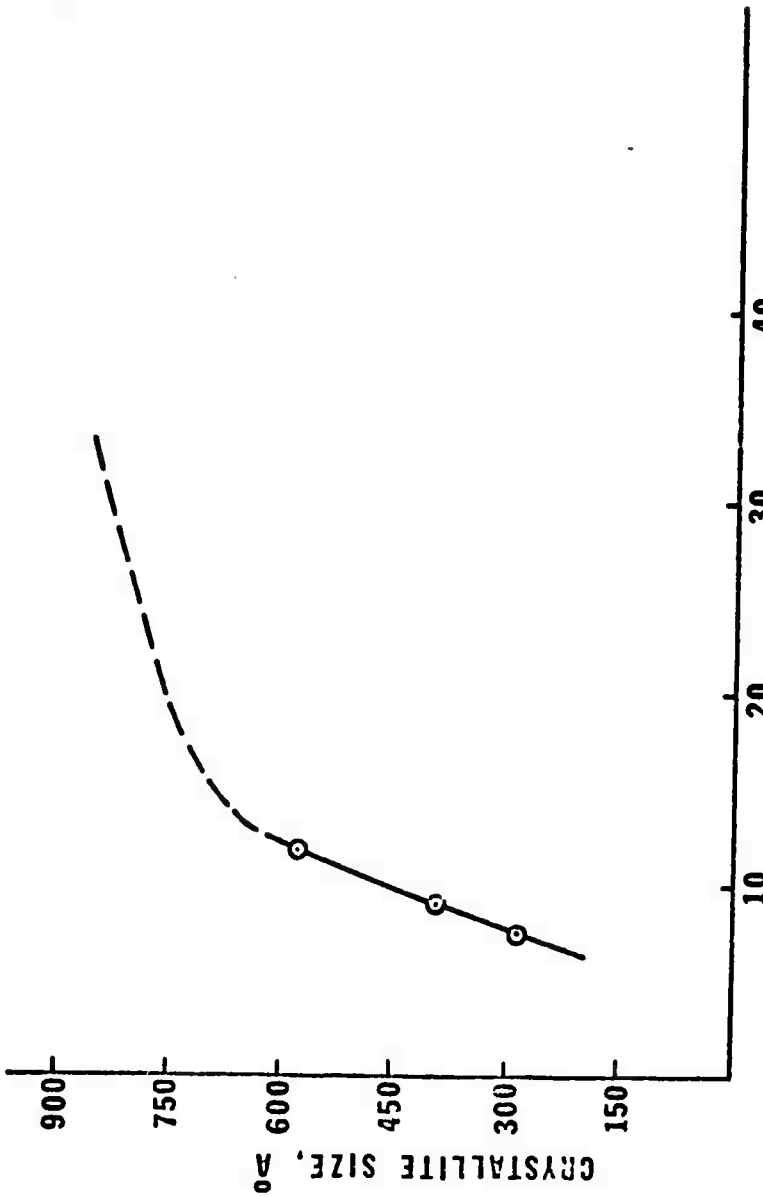

Fig. 16. Crystallite size as a function of time, from x-ray data of $GeSe_{1.5}$ held at 475°C.

were used since suitably large flat samples were frequently not available. The pressed and solid samples were first run in the Norelco diffractometer using a diffracted beam monochromator and MoKα radiation. The x-ray tube was run at 50 kv and 20 ma. Scan speed was 2° (2θ) per minute and the slit system parameters were 4°, 0.003 inches and 1/2°. The scattered intensity was measured by scintillation detector and pulse height analyzer. The diffracted beam monochromator technique has been shown* to eliminate Compton scattering at the higher angles of diffraction, when employed with Mo radiation. This is an important feature of the analysis of glasses.

Runs were also carried out using Cu radiation in a G.E. horizontal unit. This equipment has a lithium fluoride curved crystal monochromator and uses a proportional counter with a pulse height analyzer.

The x-ray data were corrected for air scattering, for polarization, and for effects arising from the monochromators. Measurements have been made on a number of compositions in the Ge-Se-As system and on $GeSe_{1.5}$ for comparison with the thin film measurements.

The corrected data was then normalized around the independent f_i^2 scattering curve, the si(s) curves were derived and were transformed following standard procedures (as

---

*R. Kaplow, S. L. Strong and B. L. Averbach, Phys. Rev., 138A, 1336 (1965); W. Ruland, Brit. J. Appl. Phys., 15, 1301 (1964).

described in earlier reports). Figures 17 through 19 show corrected x-ray intensity (Cu and Mo radiation) versus diffraction angle for samples of Ge_2Se_3As, Ge_3Se_3As, Ge_3Se_5As, respectively. The striking similarity of these curves to those obtained by electrons for the $GeSe_x$ and $As_2Se_xTe_{1-x}$ systems can be noted, particularly in respect to the diffuse ring at small s values. The curve for $GeSe_{1.5}$ is given in Fig. 20. Radial distribution functions for these curves are in preparation and will be reported at a later date.

High temperature diffraction studies. The equilibrium phase diagram for the Ge-Se system as reported by Ch'un-hua et al* indicates the existence of a GeSe phase in the temperature range 620 to 670°C. Other workers** do not show such a region. The existence or nonexistence of this phase field was examined by heat treating $GeSe_{1.5}$ glasses through the transition region.

A high temperature XRD camera (Unicam) was used. The powdered $GeSe_{1.5}$ samples were mounted in evacuated silica capillaries of 0.5 mm O.D. The camera was temperature calibrated against the known lattice constants of pure (99.999) Au. Specimens were run at room temperature, 330°C, 515°C, 600°C and 620°C. The room temperature exposure showed only

---

*L. Ch'un-hua, A. S. Pashinkin and A. V. Vovoselova, Proc. Acadm Sci. USSR, Chem. Sect., 146, 892 (1962).

**L. Ross and M. Bourgen, Can. J. Chem., 47, 2555 (1969).

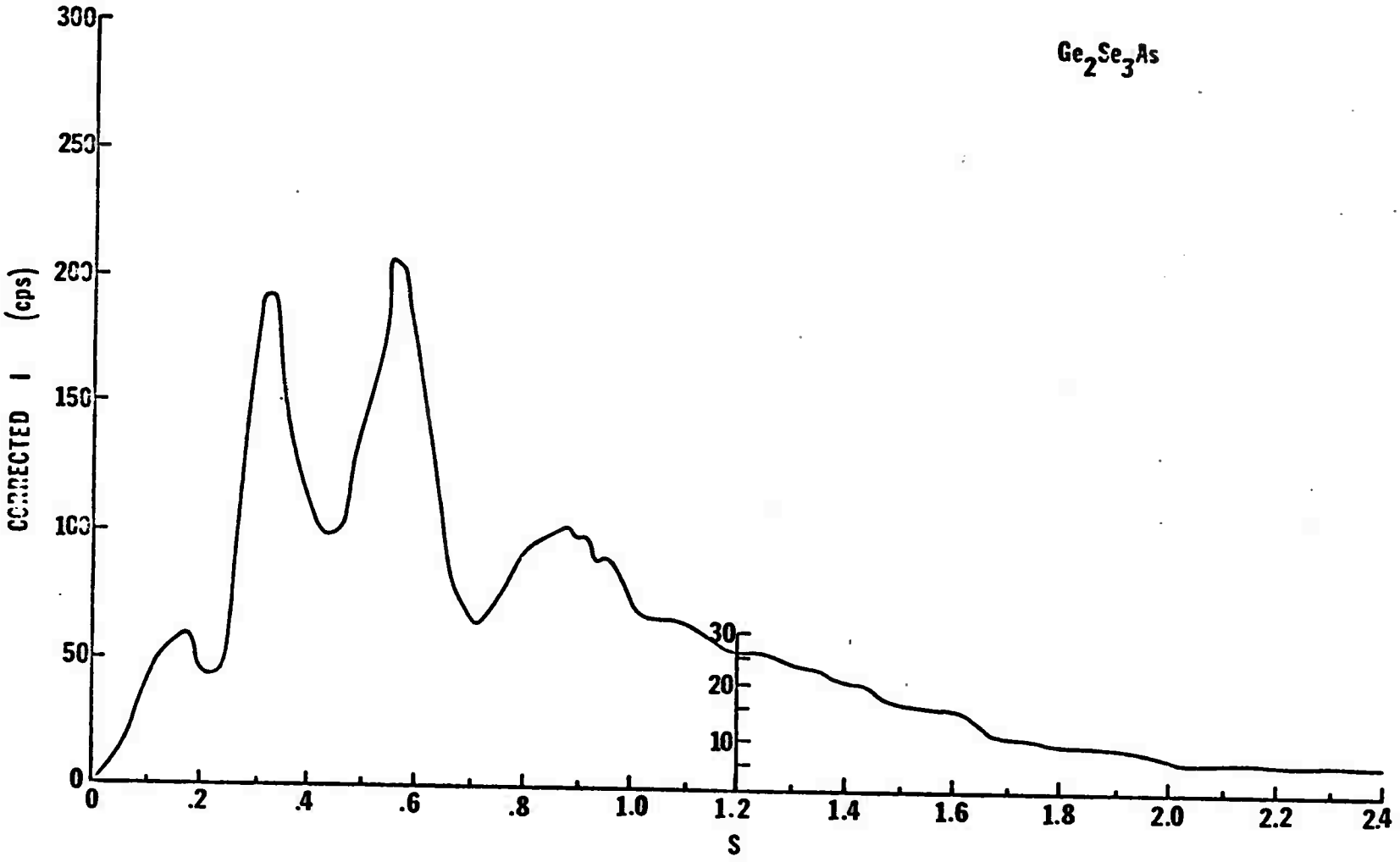

Fig. 17. Corrected x-ray intensity versus scattering angle for Ge_2Se_3As.

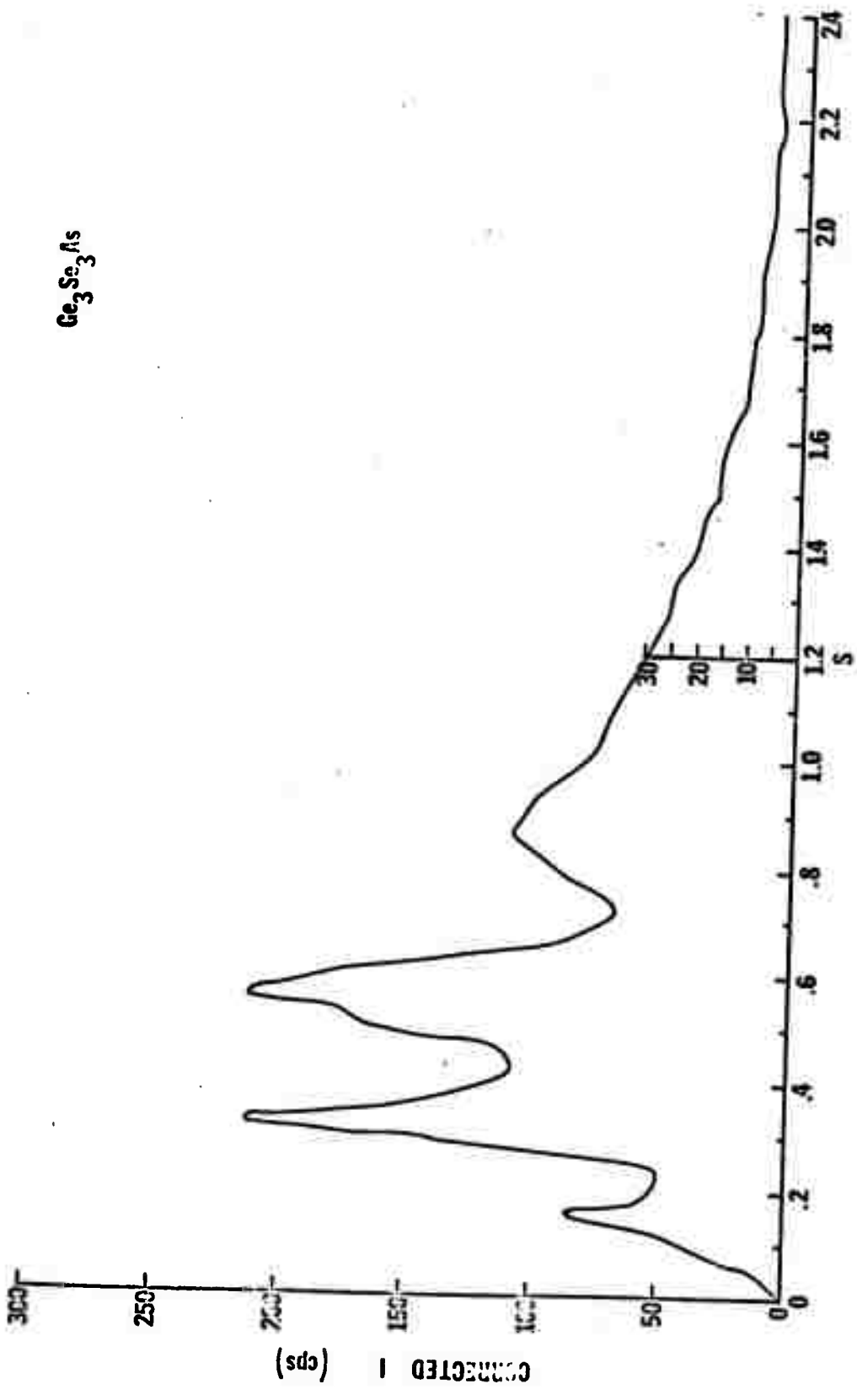

Fig. 18. Corrected x-ray intensity versus scattering angle for Ge_3Se_3As.

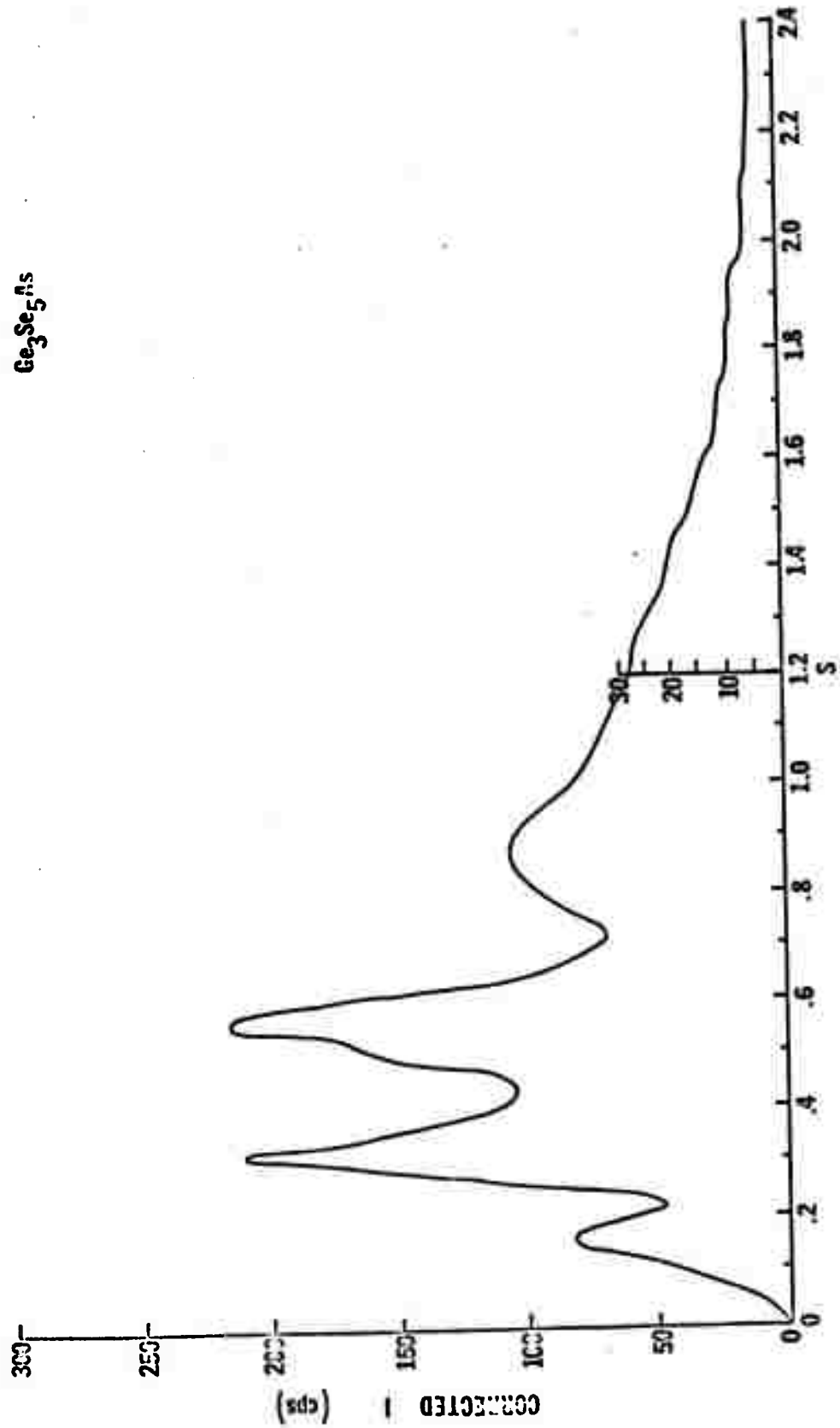

Fig. 19. Corrected x-ray intensity versus scattering angle for Ge_3Se_5As.

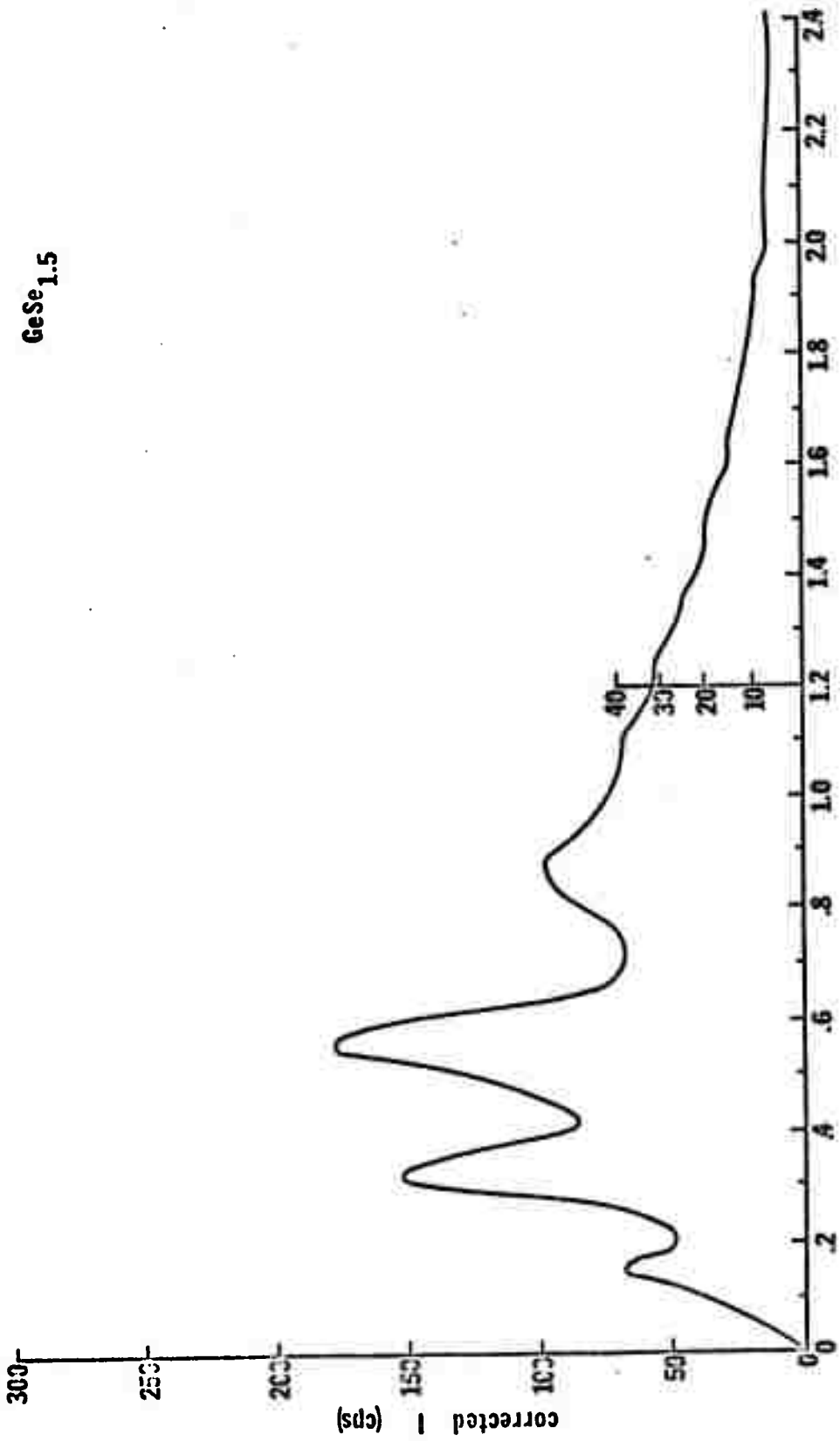

Fig. 20. Corrected x-ray intensity versus scattering angle for $GeSe_{1.5}$.

a glassy pattern typical of quenched $GeSe_{1.5}$. Exposure at 330°C and 515°C showed the two phases αGeSe and $GeSe_2$. After exposure at 620°C it was found that the specimen had remelted owing to the reduced pressure in the capillary. The specimen had separated into a ruby red glassy phase and a bright yellow crystalline $GeSe_2$ phase. In future measurements the specimen will be back-filled with argon to prevent premature melting.

Radiation effects. Samples of Ge_2AsSe_3, Ge_3AsSe_3 and $Ge_{33}As_{12}Se_{55}$ as both pressed powders and bulk solids have been submitted for high energy radiation exposure. The samples were structurally examined prior to exposure and post-irradiation structure effects will be determined upon return of the samples.

CALORIMETRIC MEASUREMENTS ON CHALCOGENIDE GLASSES

The variation in glass transition temperature (Tg) and crystallization temperature (Tc) has been studied for amorphous chalcogenides as a function of composition, impurity concentration, method of preparation and degree of radiation exposure. In addition, the enhanced crystallization seen in the TEM for thin films on Cu mesh is under investigation.

Tg's and Tc's for several compositions in the Ge-Se-As system were measured in the range 300 to 773°K with a Perkin-Elmer DSC-1B Differential Scanning Calorimeter. Scanning

taken. The spectra obtained are complex and the peaks obtained have not all been identified. Tentative results are that a two-stage process also is observed, that Se is one of the first crystallizing species, and that if the $GeSe_{1.5}$ is heated long enough only GeSe and $GeSe_2$ are present. The details are still being worked out as is the relation of these processes to the equilibrium Ge-Se phase diagram.

In the preliminary stages is a study of the enhanced crystallization that is observed with the transmission electron microscope for amorphous thin film chalcogenides on Cu mesh. A DSC scan up to 773°K for a mixture of powdered bulk $GeSe_{1.5}$ and Cu powder gave crystallization peaks identical to the pure chalcogenide. Bulk $GeSe_{1.5}$ in contact with the same Cu mesh used in TEM work likewise showed no change in crystallization behavior. In future experiments, flash evaporated $GeSe_{1.5}$ will be examined in an attempt to reproduce the conditions leading to the enhanced crystallization.

A number of samples in the Ge-Se-As system have been submitted for exposure to neutron fluxes. Identical samples retained in our laboratory will be compared with the irradiated materials to determine their radiation stability.

INFLUENCE OF ELECTRODES ON ELECTRICAL MEASUREMENTS ON SEMICONDUCTING GLASSES

In order to investigate the possibility of electrode polarization effects affecting measurements of frequency dependent properties of semiconducting glasses, a comparison has been made between electrodes in a planar (low capacitance) and sandwich (high capacitance) configuration. The two types of electrodes were prepared on the same substrate and the amorphous semiconducting material was deposited by flash evaporation, so as to cover both types of electrodes. A further deposition was then required to complete the sandwich structure.

Figure 21 shows the variation in conductance and capacitance for a Ge chalcogenide glass with planar electrodes measured at room temperature. Figure 22 shows the result when the same material is measured in a sandwich structure. Measurements were made with a General Radio bridge with the voltage across the sample adjusted to give the same voltage gradient in the glass. The sample voltage was also kept small enough to lie within the linear region of the i-v curve.

The conductance may be written

$$\sigma = \sigma_{DC} + \sigma_{AC}(\omega)$$

and the frequency dependent component is readily obtained by subtracting the DC level from the data. Figure 23 shows a plot of log σ_{AC} versus log ω for the two electrode

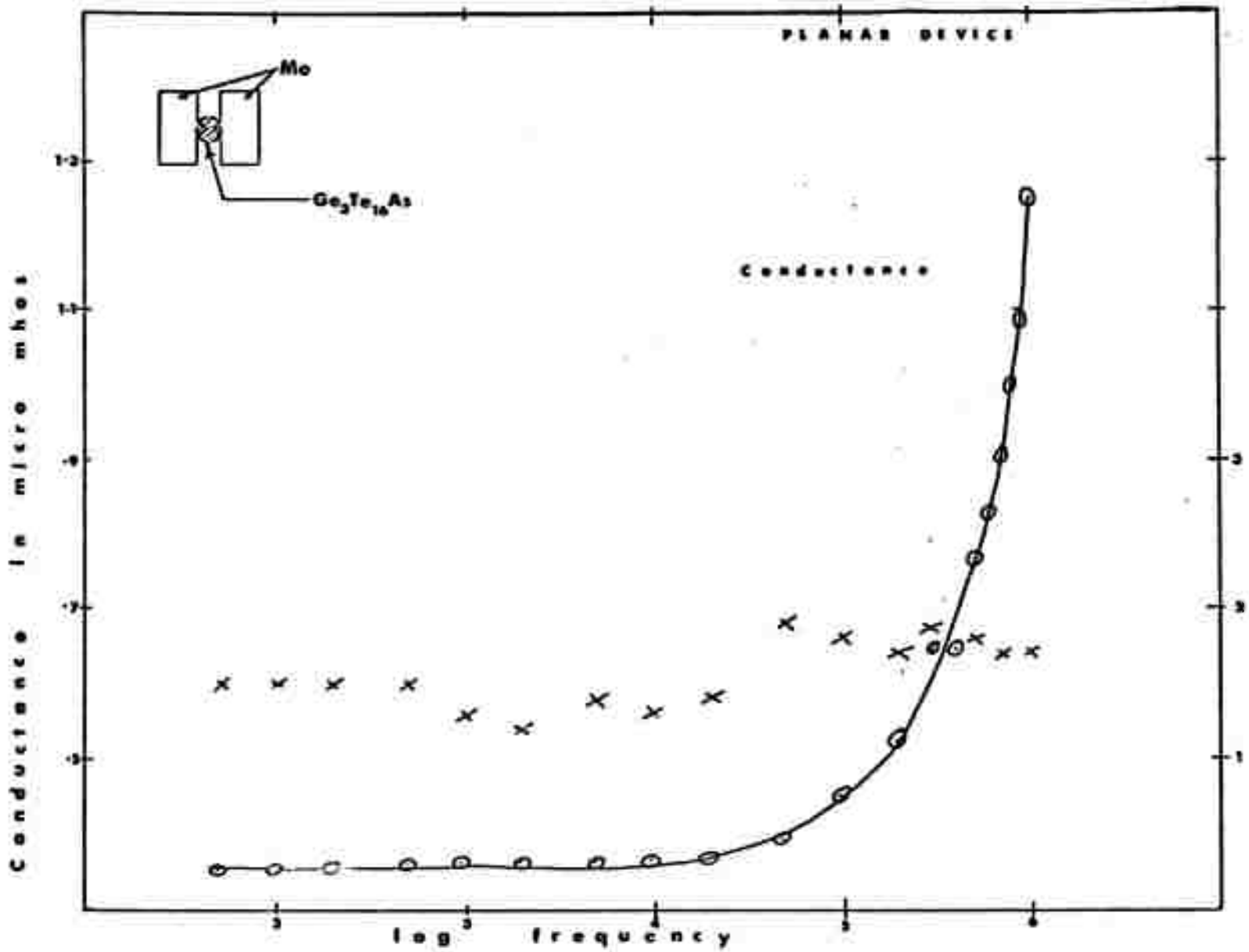

Fig. 21. Variation in conductance and capacitance for a chalcogonide glass versus frequency, measured with planar electrode geometry.

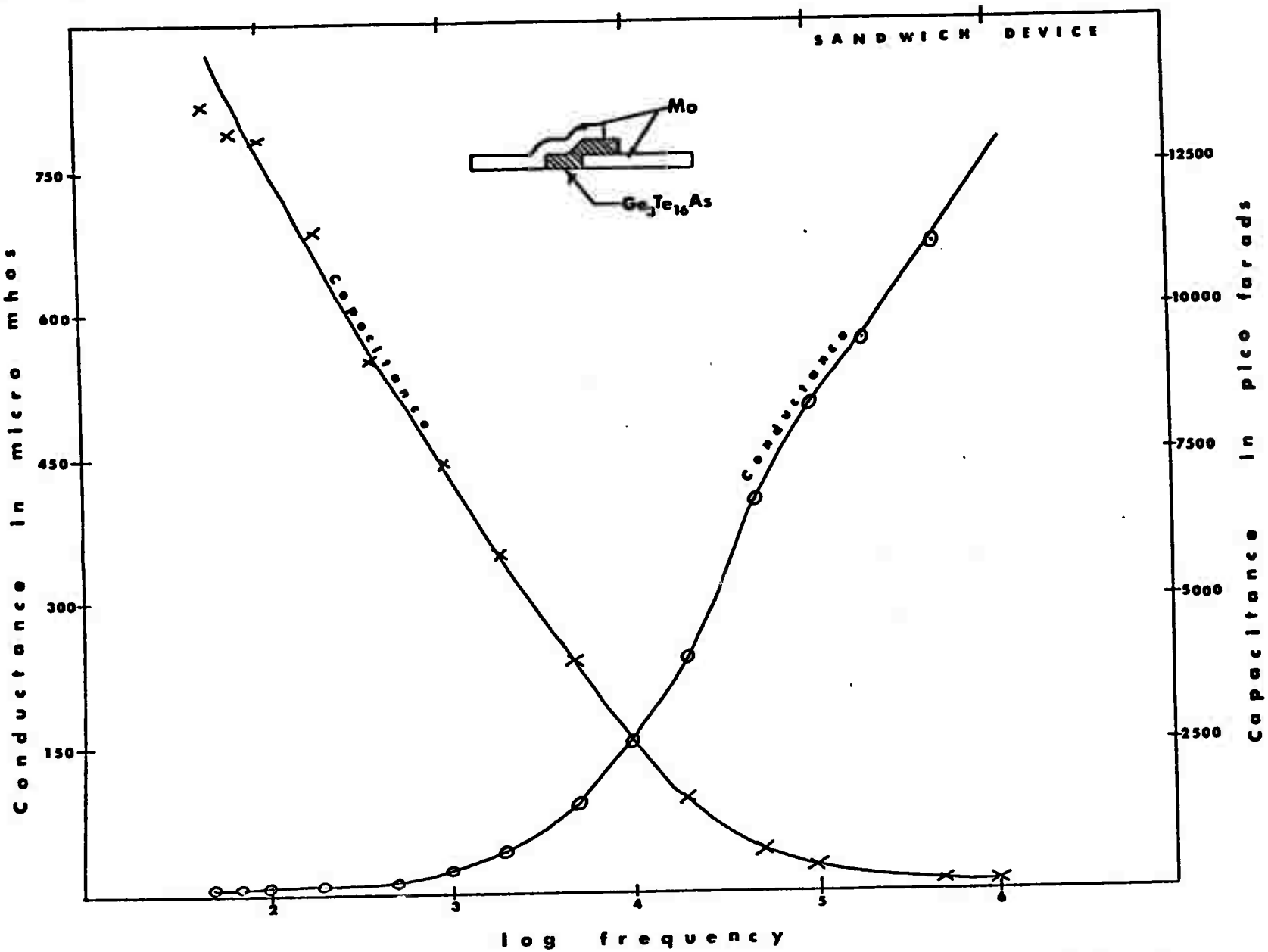

Fig. 22. Variation in conductance and capacitance for the glass of Fig. 21 measured with sandwich electrode geometry.

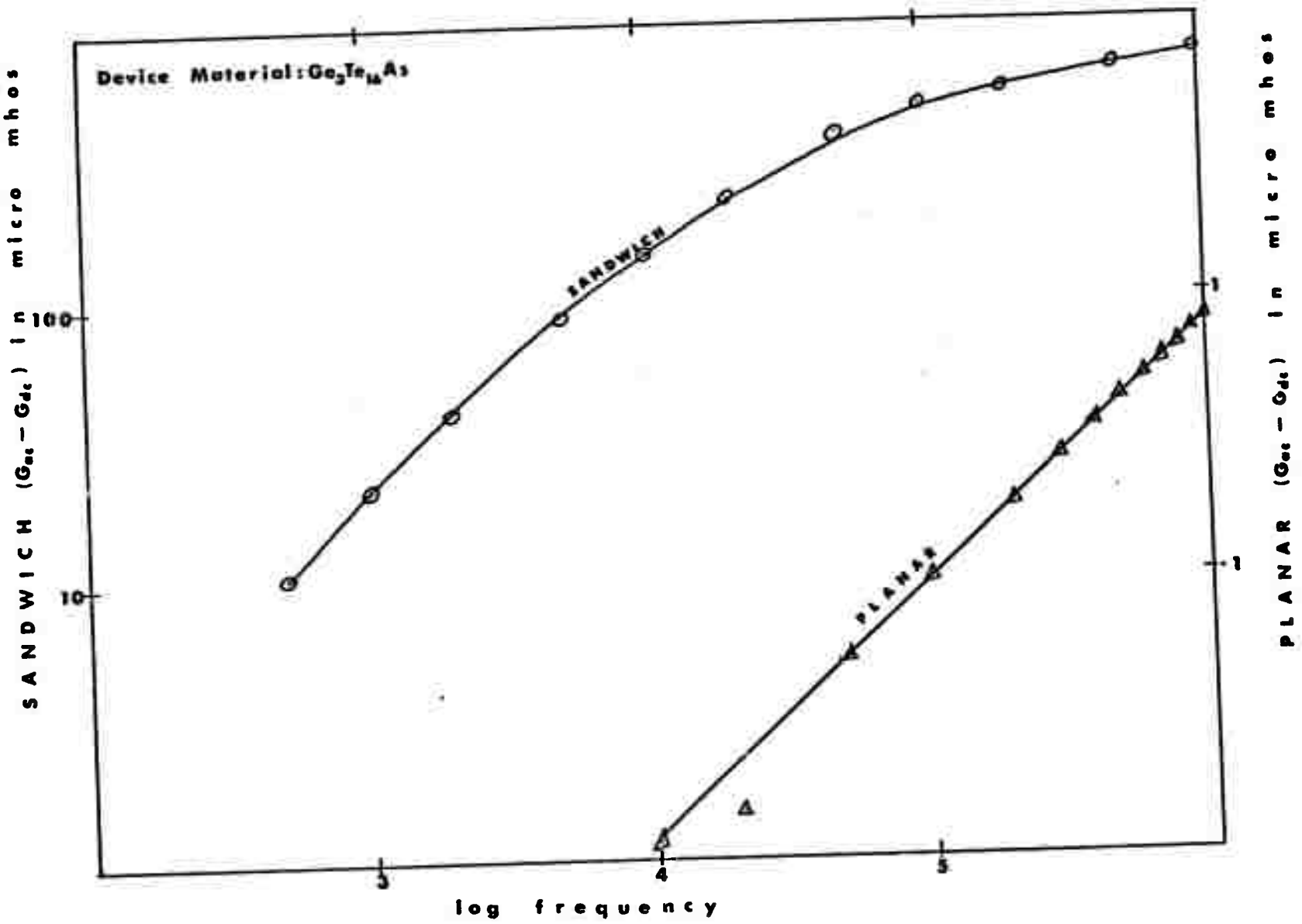

Fig. 23. Log σ_{AC} versus log ω from the data obtained with planar and sandwich electrode geometries.

configurations. In the planar case a very good $\omega^{0.8}$ dependence in agreement with the random hopping model is obtained. The sandwich configuration data, however, do not give a straight line when plotted in this way, indicating a significant electrode effect. This result has been obtained a number of times with different materials. Commonly, aluminum and molybdenum electrodes have been used.

The results are being analyzed in view of their importance for obtaining reliable measurements on the properties intrinsic to the glass and for their device implications.

PREPARATION OF REFRACTORY ELECTRODES BY THE DECOMPOSITION OF MOLYBDENUM CARBONYL

It is common experience that aluminum thin film electrodes rapidly deteriorate when used as electrodes for amorphous semiconductor switching devices. Electrodes of refractory metals appear to be relatively stable by comparison. Such electrodes are usually deposited by sputtering techniques, although it is a very slow process; deposition of a 1μ thick film of molybdenum has taken more than one hour in our laboratory. In addition, the sputtering gas must be very pure if low resistance films are to be obtained.

An alternative technique has been explored, based on the thermal decomposition of molybdenum carbonyl. This is a technique that has been employed for many years for the preparation of metals in extremely pure form. The molybdenum

carbonyl process was thoroughly discussed in a 1948 paper by Lander and Germer.* The technique has received little attention in recent years and does not appear to have been used at all for the deposition of electrodes.

Figure 24 shows a schematic of the apparatus employed for film deposition. Beneath the schematic are listed the possible reactions occurring in the decomposition of $Mo(CO)_6$. Purified argon travels through tubing to a thermostatically controlled chamber which contains a $Mo(CO)_6$ vapor injector and a plating chamber. The vapor injector is a side arm containing crystalline $Mo(CO)_6$ (a white powder) surrounded by a heater with an adjacent thermocouple. The plating chamber contains a tube for introducing the argon carrier gas and carbonyl vapor, and contains a substrate heater and a thermocouple. The outer chamber maintains its contents at a temperature high enough to prevent recondensation of the carbonyl once it is vaporized. The substrates in all cases were glass plates or Ta foil.

Table IV shows some of the conditions under which films were prepared, as well as some of their physical characteristics. Thicknesses were measured by interferometric techniques; resistances were measured using a Keithley digital multimeter and a standard electrode configuration. The main result is that it is possible to get adherent, low resistance films in a few minutes of deposition time with the substrate

---

*J. J. Lander and L. Germer, Trans. AIME, 175, 648 (1948).

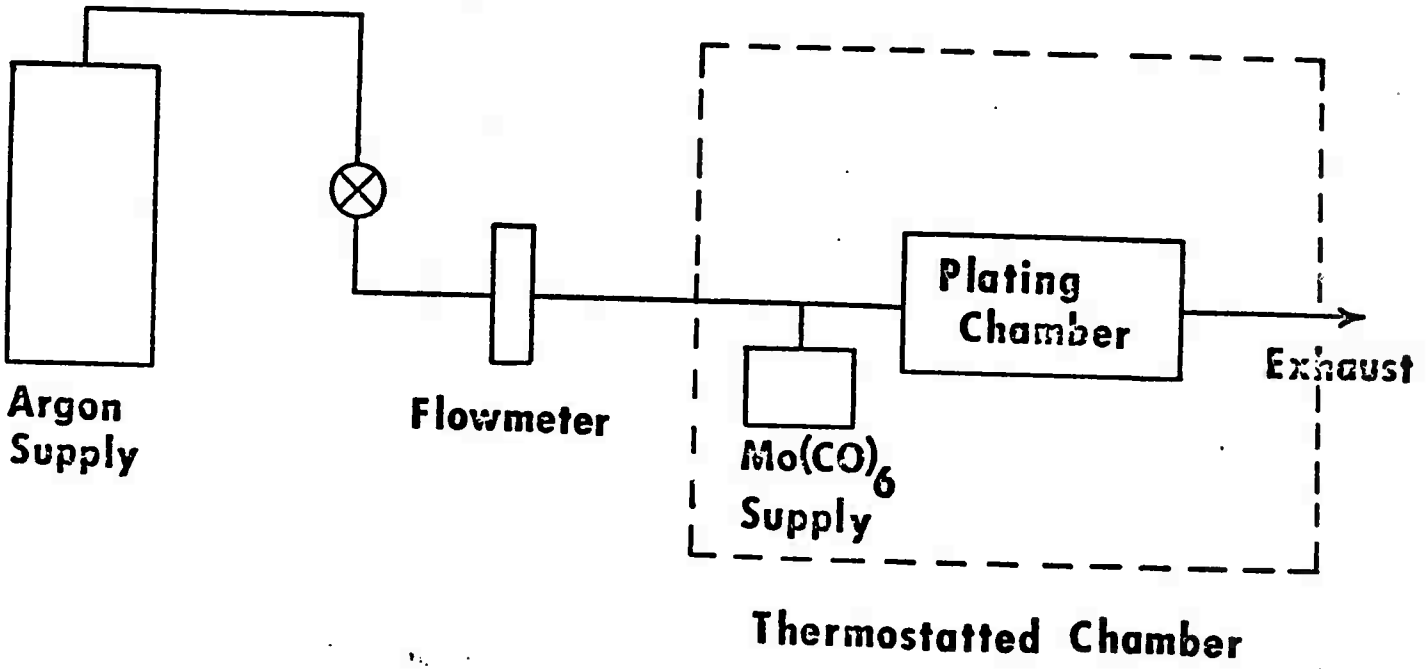

$$Mo(CO)_6 \longrightarrow Mo + 6CO\uparrow$$

$$2\ CO \longrightarrow C + CO_2\uparrow$$

$$Mo + \delta\ C \longrightarrow MoC_\delta$$

Fig. 24. System for the deposition of refractory Mo films by decomposition of molybdenum carbonyl.

Table IV

Summary of measurements on films deposited by decomposition of molybdenum carbonyl

ID #	Gas Flow Rate (scfh)	$Mo(CO)_6$ Temperature (°C)	Substrate Temperature (°C)	Time of Deposition (min.)	Thickness (Å)	Resistance (ohms)	Coherence
Mo 7a	.4	157	200	12		63	partially incoherent
7b	.4	157	200	8		33.3	coherent
7c	.4	157	200	10		63.4	coherent
Mo 8a	.4	157	250	10		19.2	coherent
8b	.4	157	175	10		1.9MΩ	thin coherent
8c	.4	157	250	10	2,212.5 1,751.1	6.5 40	coherent incoherent
8f	.4	157	200	10		13.6	incoherent
8g	.4	157	200	8	1,622.5	740	coherent
8h	.4	157	200	9	2,212.5	76	partially coherent
Mo 9a	.4	132	200	15		5,500	coherent
9b	.4	110	200	15	860.4	240KΩ	coherent some oxidation

temperature no higher than 250°C.

Although the films were shiny and metallic in appearance, decomposition of CO to CO_2 and C during deposition allows the possibility of carbide formation. Figure 25 shows a series of typical x-ray spectra for these films. It was found that the deposited films were consistently x-ray amorphous. Heat treatments at temperatures up to the softening point of the substrate produced no crystallization. The depositions were repeated onto Ta foil to permit heat treatments at higher temperatures as shown in Fig. 25. Finally, crystallization was observed and a spectrum obtained which showed the presence of Mo and Mo_2C in about a 2:1 ratio. Carbide formation may actually be advantageous for the present application since Mo_2C would be expected to be even less reactive chemically than pure Mo. Figure 26a (550X) and Fig. 26b (1,870X) are scanning electron micrographs of the Mo-Mo_2C film after it flaked off the Ta due to the severe thermal cycling after heat treatment.

Examination of samples in the transmission electron microscope also showed them to be initially amorphous, although it was possible to produce crystallization by beam heating. An electron diffraction RDF scan has been made and the data are being analyzed.

In summary, refractory electrodes have been deposited with good conductivity and satisfactory thickness, requiring only a few minutes' deposition and utilizing very simple

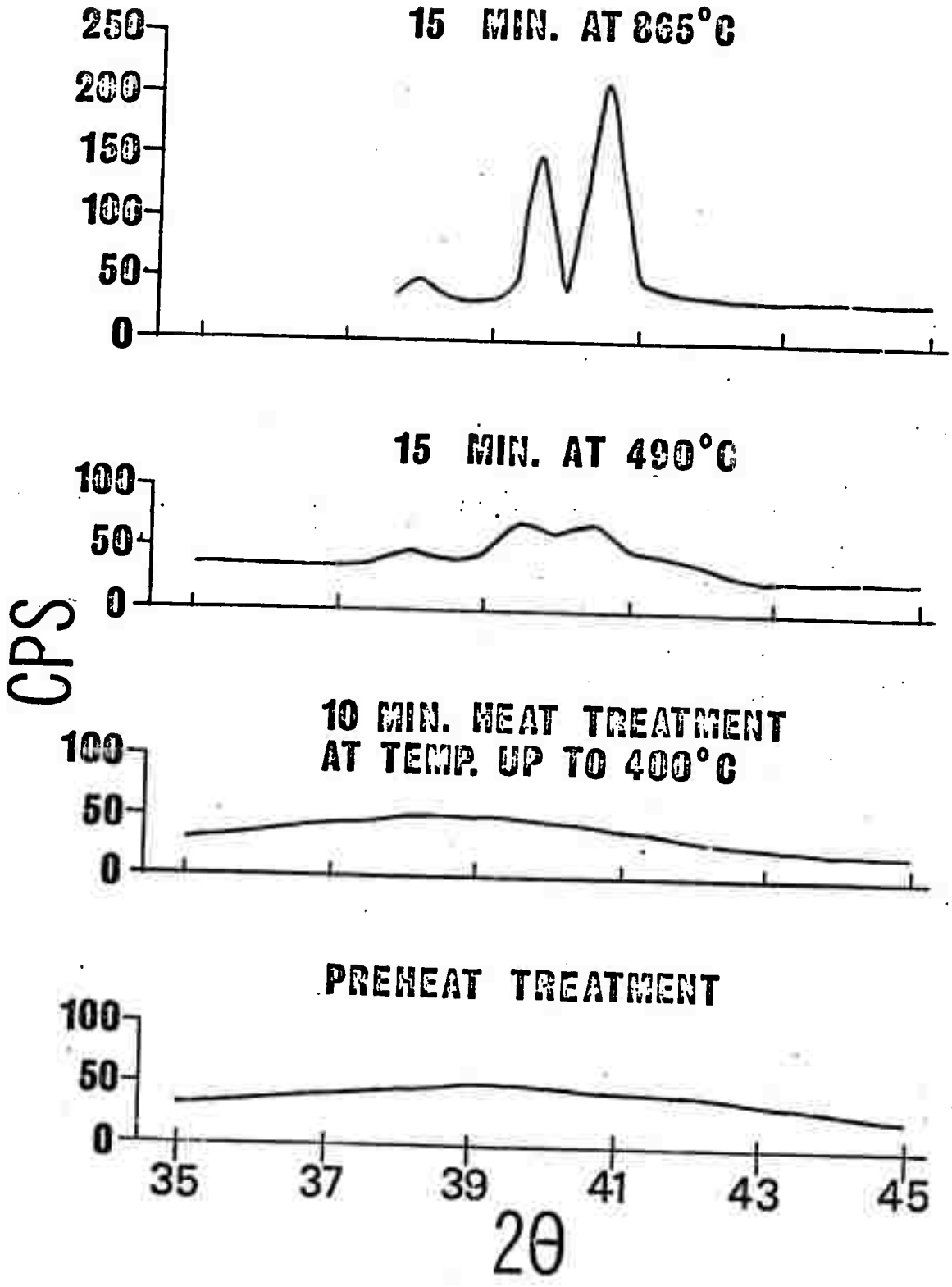

Fig. 25. X-ray traces showing effect of heat treatment on the films deposited by decomposition of molybdenum carbonyl.

(a)

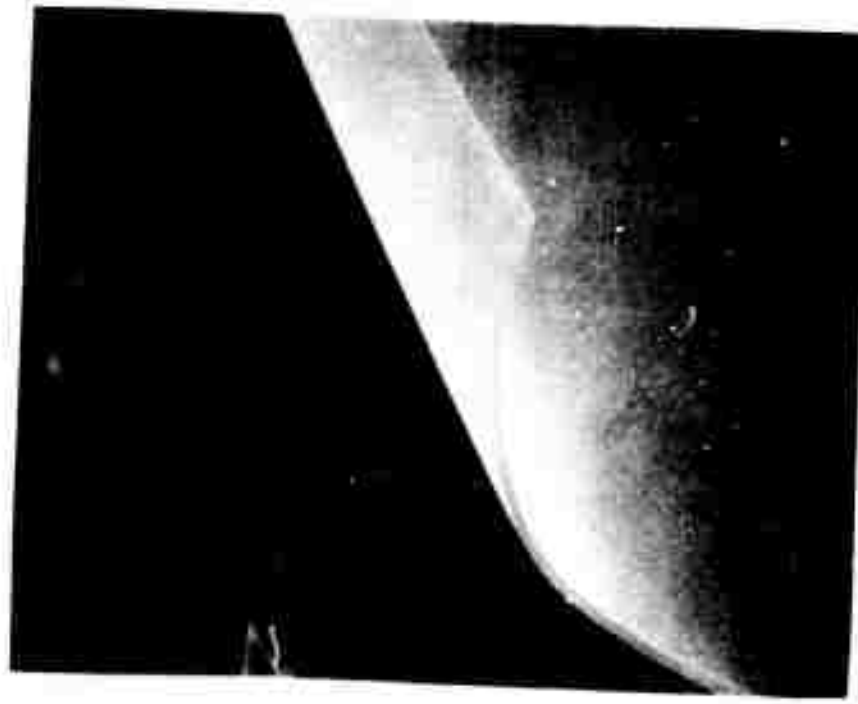

(b)

Fig. 26. Scanning electron micrographs (a) at 550X and (b) at 1,870X of an Mo-MoSi$_2$ film flaked from a Ta substrate after severe thermal cycling.

off-the-shelf chemical apparatus. A possible disadvantage is the necessity to hold the substrate at 200 to 250°C during deposition.

ACKNOWLEDGEMENTS

Acknowledgements are due to research assistants A. Armstrong, J. Chang, A. DeRosa, D. Firestone, R. Irani and B. Molnar for their valuable contributions to this project.

Security Classification

DOCUMENT CONTROL DATA - R & D

(Security classification of title, body of abstract and indexing annotation must be entered when the overall report is classified)

1 ORIGINATING ACTIVITY (Corporate author)
University of Florida
Engineering & Industrial Experiment Station
Gainesville, Florida 32601

2a. REPORT SECURITY CLASSIFICATION
Unclassified

2b. GROUP

3 REPORT TITLE
STRUCTURE, PROPERTIES AND RADIATION SENSITIVITY OF ELECTRICALLY BISTABLE MATERIALS

4. DESCRIPTIVE NOTES (Type of report and inclusive dates)
Technical Report, 2nd Annual, 6 February 1971 to 6 February 1972

5. AUTHOR(S) (First name, middle initial, last name)
Derek B. Dove, Larry L. Hench, Robert W. Gould and Ronald E. Loehman

6. REPORT DATE	7a. TOTAL NO. OF PAGES	7b. NO. OF REFS
6 February 1972	51	-

8a. CONTRACT OR GRANT NO.	9a. ORIGINATOR'S REPORT NUMBER(S)
DAHC04-70-C-0024	Technical Report No. 4
b. PROJECT NO. P-8993-P	9b. OTHER REPORT NO(S) (Any other numbers that may be assigned this report)
c.	
d.	

10 DISTRIBUTION STATEMENT

11. SUPPLEMENTARY NOTES	12. SPONSORING MILITARY ACTIVITY
This research was supported by Advanced Research Projects Agency	Army Research Office, Durham

13. ABSTRACT

This second annual report describes work carried out on the structural and electrical characterization of chalcogenide glasses. Electron diffraction radial distribution studies have been completed in the $As_2Te_{3-x}Se_x$ system and the thermal stability of these glasses in the presence of metallic surface layers has been examined. X-ray measurements on the kinetics of crystallization of bulk $GeSe_x$ glasses have been continued and diffuse scattering data have been obtained on a number of Ge-Se-As bulk glasses. Glass transition and crystallization temperatures have been observed by differential scanning calorimetry, a technique of high sensitivity.

A comparison is made between the a.c. conductivity of glasses measured with planar and sandwich electrode configurations. A significant difference has been found which may be attributed to electrode polarization effects in the sandwich structure.

Finally, a simple technique employing the decomposition of molybdenum carbonyl is described for the rapid deposition of thick refractory electrodes of good conductivity.

DD FORM 1 NOV 65 1473

Security Classification

14 KEY WORDS	LINK A		LINK B		LINK C	
	ROLE	WT	ROLE	WT	ROLE	WT
Amorphous semiconductors Radial Distribution Analysis Thin film devices Electrode effects Thermal treatment						